© 2015. Published by The Company of Biologists Ltd | Journal of Cell Science (2015) 128, 4293-4305 doi:10.1242/jcs.164509

RESEARCH ARTICLE

Cdc42 regulates epithelial cell polarity and cytoskeletal function during kidney tubule development

Bertha C. Elias[1], Amrita Das[2], Diptiben V. Parekh[1], Glenda Mernaugh[1], Rebecca Adams[1], Zhufeng Yang[2], Cord Brakebusch[3], Ambra Pozzi[1,4,5], Denise K. Marciano[2], Thomas J. Carroll[2,6] and Roy Zent[1,4,7,*]

ABSTRACT

The Rho GTPase Cdc42 regulates key signaling pathways required for multiple cell functions, including maintenance of shape, polarity, proliferation, migration, differentiation and morphogenesis. Although previous studies have shown that Cdc42 is required for proper epithelial development and maintenance, its exact molecular function in kidney development is not well understood. In this study, we define the specific role of Cdc42 during murine kidney epithelial tubulogenesis by deleting it selectively at the initiation of ureteric bud or metanephric mesenchyme development. Deletion in either lineage results in abnormal tubulogenesis, with profound defects in polarity, lumen formation and the actin cytoskeleton. Ultimately, these defects lead to renal failure. Additionally, *in vitro* analysis of Cdc42-null collecting duct cells shows that Cdc42 controls these processes by regulating the polarity Par complex (Par3–Par6–aPKC–Cdc42) and the cytoskeletal proteins N-Wasp and ezrin. Thus, we conclude that the principal role of Cdc42 in ureteric bud and metanephric mesenchyme development is to regulate epithelial cell polarity and the actin cytoskeleton.

KEY WORDS: Ureteric bud, Metanephric mesenchyme, GTPase, Signaling, Epithelial cell

INTRODUCTION

Mammalian kidney development begins when the ureteric bud invades the surrounding metanephric mesenchyme (Carroll and Das, 2013; Costantini and Kopan, 2010; Dressler, 2006). The ureteric bud is induced to undergo iterative rounds of branching morphogenesis and gives rise to the collecting system, whereas the metanephric mesenchyme forms the nephrons that consist of the glomeruli and renal tubules. Reciprocal signaling between the ureteric bud and the metanephric mesenchyme is required for ureteric bud branching morphogenesis and metanephric mesenchyme development.

Cdc42, a member of the Rho GTPases, plays a crucial role in regulating multiple cell functions including cell shape, polarity, proliferation, invasion, migration and differentiation (Melendez et al., 2011). Cdc42 mediates these functions by controlling cytoskeletal dynamics due to its ability to interact with the Wiskott–Aldrich syndrome protein (Wasp) and p21-activated kinases (PAKs). Wasp regulates actin polymerization and filopodia formation through direct interactions with both profilin and actin, and PAKs alter the activity of the crucial actin-binding protein cofilin (Melendez et al., 2011). In addition, Cdc42 regulates epithelial cell polarity by forming complexes with the PAR protein family, atypical protein kinase C (aPKC) and cadherins (Goldstein and Macara, 2007).

Both *in vitro* and *in vivo* evidence suggest a crucial role for Cdc42 in kidney development. Cdc42 is required by Madin–Darby canine kidney (MDCK) cells to form tubules in three-dimensional (3D) culture by regulating the formation of the apical plasma membrane domain and tight junctions as well as primary ciliogenesis (Choi et al., 2013; Kim et al., 2007; Martin-Belmonte et al., 2007; Rodriguez-Fraticelli et al., 2010; Rogers et al., 2003; Zhang et al., 2001; Zuo et al., 2011). Two studies have shown that Cdc42 is essential for normal kidney development and function. In the first, Cdc42 deletion from renal tubular epithelia with the Ksp-cre (which causes cre-mediated recombination in developing nephrons and the renal collecting system) was shown to result in lethal cystic kidney disease that was attributed to abnormalities in ciliogenesis (Choi et al., 2013). In a second study, Cdc42 was deleted in the nephron progenitors using Six2-cre. These mice formed hypoplastic kidneys with a reduced nephrogenic zone and small papillae (Reginensi et al., 2013). This phenotype was attributed to defects in localization of the transcriptional activator Yap. Although both studies demonstrate roles for Cdc42 in kidney development, their proposed mechanisms of action for Cdc42 are different and out of keeping with its principal function as a master regulator of the actin cytoskeleton and a mediator of epithelial cell polarity.

There is little known about how apical-basal polarity is established during renal tubulogenesis. Afadin, an F-actin-binding and nectin adaptor protein, has been shown to be essential for the timely initiation of apical-basal polarity during epithelialization of developing nephrons (Yang et al., 2013). In addition, this adaptor protein is essential for the formation of a continuous apical surface and lumen formation (Yang et al., 2013). At the molecular level, absence of afadin in developing nephrons results in a delayed lumen formation and a reduced ability to correctly localize members of the Par complex (Par3–Par6–aPKC–Cdc42; in mammals, Par3 is also known as PARD3 and Par6 as PARD6, with each having two isoforms) to the forming epithelia, suggesting that defects in Par complex function and Cdc42 activation might be the underlying defect. Afadin is necessary for Cdc42 activation *in vitro* (Kawakatsu et al., 2002; Kurita et al., 2013; Mandai et al., 2013; Nakanishi and Takai, 2004), suggesting that the principal mechanisms whereby Cdc42 regulates tubulogenesis in the kidney might be by altering the actin cytoskeleton and apical-basal polarity of the epithelial cells.

[1]Division of Nephrology and Hypertension, Department of Medicine, Vanderbilt University School of Medicine, Nashville, TN 37232, USA. [2]Department of Medicine, University of Texas Southwestern Medical Center, Dallas, TX 75390, USA. [3]Biotech Research Center, University of Copenhagen, Ole Maaløes Vej 5, Copenhagen DK-2200, Denmark. [4]Department of Cancer Biology, Vanderbilt University School of Medicine, Nashville, TN 37232, USA. [5]Veterans Affairs Hospital, Nashville, TN 37232, USA. [6]Department of Molecular Biology, University of Texas Southwestern Medical Center, Dallas, TX 75390, USA. [7]Department of Cell and Developmental Biology, Vanderbilt University School of Medicine, Nashville, TN 37232, USA.

*Author for correspondence (roy.zent@vanderbilt.edu)

Received 10 October 2014; Accepted 14 October 2015

Journal of Cell Science (2015) 128, 4293-4305 doi:10.1242/jcs.164509

Given the discrepant findings of Cdc42 function in renal epithelial tubulogenesis compared to its demonstrated function in other epithelia, and the recent findings suggesting that afadin regulates Cdc42 and renal epithelial cell polarity, we investigated the role of Cdc42 in the developing kidney, focusing on its role in establishing apical-basal polarity and in cytoskeletal architecture. We used Cdc42$^{flox/flox}$ mice crossed with two different cre deletor strains; Six2-cre and Hox-B7-cre. Six2-cre deletes Cdc42 in the cap mesenchyme of the metanephric mesenchyme and was used in one of the prior studies (Reginensi et al., 2013). Hoxb7-cre deletes Cdc42 in the ureteric bud, which gives rise to the collecting system starting at embryonic day (E)10.5. We show that Cdc42 is required for both ureteric bud and metanephric mesenchyme development as the Hoxb7-cre:Cdc42$^{flox/flox}$ mice develop a severe branching morphogenesis defect, and Six2-cre:Cdc42$^{flox/flox}$ mice are unable to form nephrons. Both mice have serious abnormalities in epithelial cell polarization at all developmental stages examined. In particular, the Six2-cre:Cdc42$^{flox/flox}$ kidney phenotype is highly reminiscent of the afadin mutants with disruption of Par complex formation and discontinuous lumens. Using Cdc42-null collecting duct cells, we showed that absence of Cdc42 caused profound adhesion, migration, and polarization defects, as well as marked reduction in N-Wasp (also known as WASL) and ezrin activation. Thus, we conclude that a primary function of Cdc42 in the formation of kidney tubules is to promote epithelial cell polarization through Par complex formation and to regulate cytoskeletal architecture through a Cdc42–N-Wasp–ezrin signaling pathway.

RESULTS

Cdc42 is required for ureteric bud development

We crossed Hoxb7-cre mice, which express cre recombinase in the Wolffian duct and ureteric bud from E10.5 onwards, with Cdc42$^{flox/flox}$ mice to define the role of Cdc42 in the developing ureteric bud. The mice were born in the predicted Mendelian ratio; however, all the Hoxb7-cre:Cdc42$^{flox/flox}$ mice died by four weeks of age. Cdc42 deletion was confirmed in mutant mice by performing immunohistochemistry on E15 embryos (Fig. 1A,B) and immunoblotting on isolated papillae of newborn Hoxb7-cre:Cdc42$^{flox/flox}$ with an antibody directed at Cdc42 (Fig. 1C). The kidneys of the Hoxb7-cre:Cdc42$^{flox/flox}$ mice were much smaller than their wild-type controls and had histological features of end-stage renal disease characterized by severe destruction of the cortex and medulla (Fig. 1D–I). When Hoxb7-cre:Cdc42$^{flox/flox}$ mice were killed prior to end-stage renal failure; there was relative preservation of the cortex compared to the severe tubular abnormalities in the medulla. The markedly decreased number of tubules found within the renal papilla of the dysmorphic dysplastic Hoxb7-cre:Cdc42$^{flox/flox}$ kidneys were consistent with a major branching

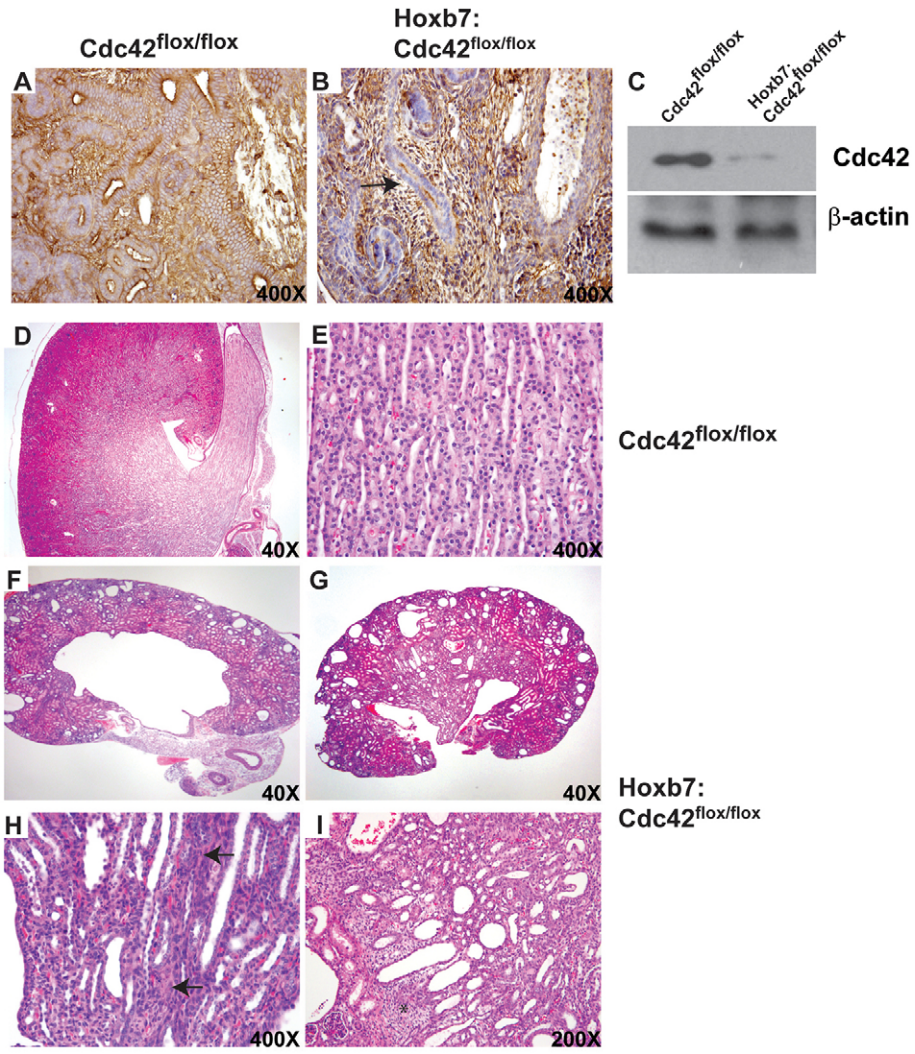

Fig. 1. Hoxb7-cre:Cdc42$^{flox/flox}$ mice develop end-stage renal failure due to defective branching morphogenesis and intraluminal obstruction in the collecting ducts. (A–C) Sections of E15.5 mouse kidneys from Cdc42$^{flox/flox}$ and Hoxb7-cre:Cdc42$^{flox/flox}$ mice were stained with antibodies directed against Cdc42. No Cdc42 was visualized in the developing ureteric bud (arrow) of Hoxb7-cre:Cdc42$^{flox/flox}$ mice (A,B). Deletion of Cdc42 in the Hoxb7-cre:Cdc42$^{flox/flox}$ mice was confirmed by immunoblotting the kidney papilla of newborn mice with an anti-mouse Cdc42 antibody (C). (D–I) Microscopy of hematoxylin and eosin (H&E)-stained kidney slides showing destruction of the medulla and corticomedullary junction in Hoxb7-cre:Cdc42$^{flox/flox}$ but not in the Cdc42$^{flox/flox}$ kidneys. Total destruction of the medulla due to hydronephrosis in Hoxb7-cre:Cdc42$^{flox/flox}$ mice is present just prior to death at 4 weeks of age (F); at 2 weeks of age the kidneys are severely hypoplastic and dysplastic with dilated tubules found within the cortex and medulla and evidence of focal tubular cysts (G). High power images (H) show the medulla where the lumens of the collecting ducts are filled with cells (arrows) and the tubules are dilated. Dilated tubules and interstitial fibrosis (*) are seen in the cortex (I). The magnification at which the images were viewed is displayed.

Journal of Cell Science (2015) 128, 4293-4305 doi:10.1242/jcs.164509

morphogenesis defect (Fig. 1G). Many lumens of the collecting ducts were not apparent (marked by arrows in Fig. 1H) and there were also areas of marked interstitial fibrosis between the dilated cortical collecting ducts (marked by * in Fig. 1I).

We next defined when the branching defect in the mice began by performing histological studies of kidneys at various embryonic stages. As early as E12.5, there were fewer ureteric bud structures (marked by arrows) and less metanephric mesenchyme induction in mutants compared to wild type (Fig. 2A,B). This became more evident over time. The mutant ureteric bud was very poorly formed at E15.5 (Fig. 2C,D) and E18.5 (Fig. 2E,F) with fewer nephrons at both these time points. The branching defect was confirmed by calbindin staining at E18.5 (Fig. 2G,H). To define why the kidneys of the Hoxb7-cre:Cdc42$^{flox/flox}$ mice were hypoplastic, we quantified proliferation and apoptosis in the kidney. Interestingly there was no statistical difference in proliferation of the cytokeratin-positive ureteric bud cells in the Hoxb7-cre:Cdc42$^{flox/flox}$ kidneys as defined by staining for phosphorylated histone H3 (pHH3) at E13.5, E15.5 or E18.5 (Fig. 2I–K). In contrast, when we assessed proliferation of Six2 positive cells at E18.5, there was a 60% decrease in the Hoxb7-cre:Cdc42$^{flox/flox}$ kidneys (Fig. 2I,J,L) and this difference was also seen in newborn mice (data not shown). There was no difference in apoptosis rates between the two genotypes at any time points (data not shown). Thus, deletion of Cdc42 in the developing ureteric bud caused a severe ureteric bud branching defect and secondarily impaired cell proliferation within the metanephric mesenchyme, which presumably contributed to the reduced kidney size.

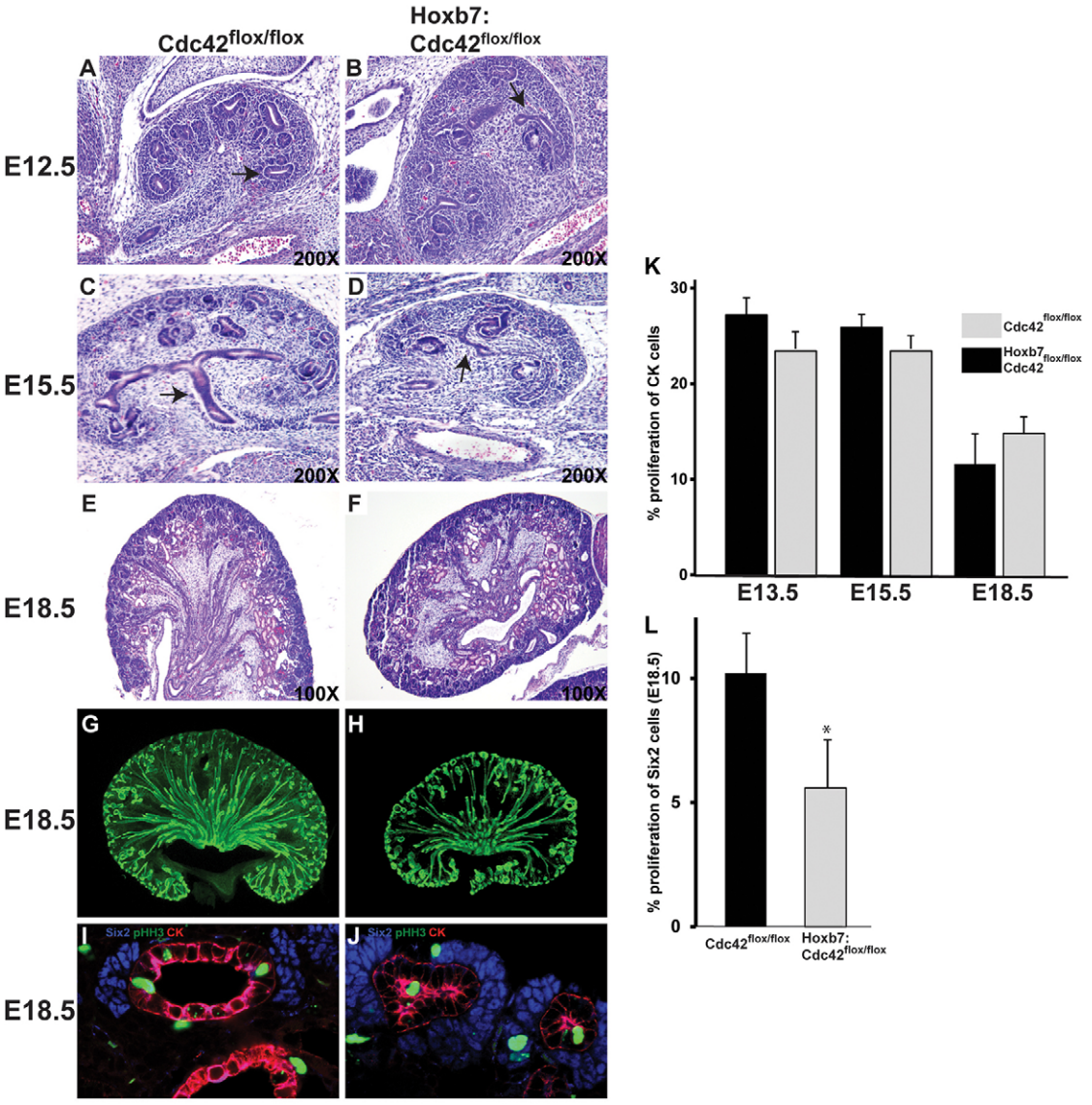

Fig. 2. Hoxb7-cre:Cdc42$^{flox/flox}$ mice have a severe branching morphogenesis defect and impaired metanephric mesenchyme induction. (A–H) Kidneys were isolated from embryos of the Cdc42$^{flox/flox}$ and the Hoxb7-cre:Cdc42$^{flox/flox}$ mice at E12.5 (A,B), E15.5, (C,D) and E18.5 (E–J). A marked ureteric bud branching morphogenesis defect (arrows) and decreased metanephric mesenchyme induction was noted at each of these time points. Calbindin staining demonstrated a decrease in ureteric bud structures at E18.5 in the Hoxb7-cre:Cdc42$^{flox/flox}$ mice when compared to the Cdc42$^{flox/flox}$ mice (G,H). pHH3 staining was performed on cytokeratin-positive cells (marking ureteric bud structures, red) and Six2-positive cells (marking metanephric mesenchyme structures, blue) (I,J). The percentage of proliferation at different time points in the ureteric bud (K) and metanephric mesenchyme (L) was quantified (mean±s.d., at least three mice were examined per group). *P<0.05 for differences between Cdc42$^{flox/flox}$ and the Hoxb7-cre:Cdc42$^{flox/flox}$ in the Six2-positive cells (Student's t-test). The magnification at which the images were viewed is displayed.

Journal of Cell Science (2015) 128, 4293-4305 doi:10.1242/jcs.164509

Cdc42 is required for metanephric mesenchyme development

Cdc42 was deleted from the metanephric mesenchyme by crossing the Cdc42$^{flox/flox}$ with the Six2-cre mouse. Six2 is expressed in the cap mesenchyme and this Cre line deletes floxed genes from all components of the developing nephron extending from the glomerular epithelium to the connecting segment (Kobayashi et al., 2008). We verified that Cdc42 was deleted in the developing metanephric mesenchyme by performing immunoblotting and immunohistochemistry on post-natal day (P) 1 Cdc42$^{flox/flox}$ and Six2-cre:Cdc42$^{flox/flox}$ mice (Fig. 3A–C). Staining revealed clearly decreased Cdc42 expression in the

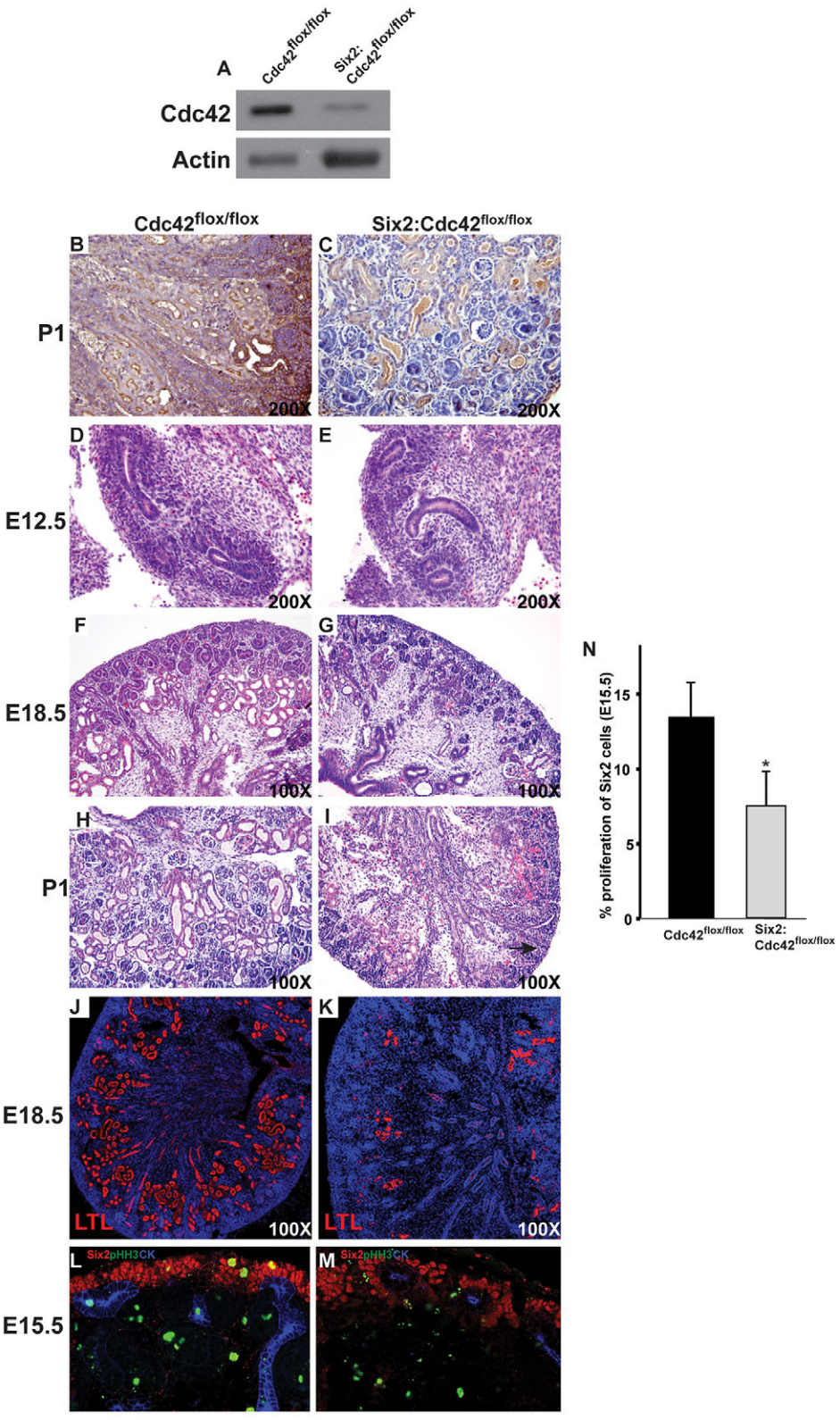

Fig. 3. Six2-cre:Cdc42$^{flox/flox}$ mice have a defect in metanephric mesenchyme development. (A) Deletion of Cdc42 in the Six2-cre:Cdc42$^{flox/flox}$ mice was confirmed by immunoblotting extracts from the kidney cortex of newborn mice with an anti-mouse-Cdc42 antibody. (B,C) No staining with an anti-Cdc42 antibody was seen in the metanephric mesenchyme of newborn Six2-cre:Cdc42$^{flox/flox}$ mice. (D,E) No ureteric bud branching defect was seen in the E12.5 Six2-cre:Cdc42$^{flox/flox}$ mice. (F–I) Diminished metanephric mesenchyme development was seen in E18.5 Six2-cre:Cdc42$^{flox/flox}$ mice (F,G), which was even more severe at P1 (H,I) with almost no nephrons formed (arrow) in the metanephric mesenchyme. (J,K) The diminished metanephric mesenchyme development was verified in E18.5 Six2-cre:Cdc42$^{flox/flox}$ kidneys as decreased lotus tetragonolobus lectin (LTL), a marker of proximal tubules, staining. (L–N) pHH3 staining was performed on Six2-positive cells of E15.5 kidneys from Cdc42$^{flox/flox}$ (L,M) and the Six2-cre:Cdc42$^{flox/flox}$ mice and quantified (mean±s.d., at least three mice were examined per group) (N). *P<0.01 for differences between Cdc42$^{flox/flox}$ and the Six2-cre:Cdc42$^{flox/flox}$ (Student's t-test). The magnification at which the images were viewed is displayed.

Journal of Cell Science (2015) 128, 4293-4305 doi:10.1242/jcs.164509

cortical kidney tissue of Six2-cre:Cdc42$^{flox/flox}$ mice. Because all the Six2-cre:Cdc42$^{flox/flox}$ mice died within 24 h of birth, we defined when the kidney abnormalities first became evident. Although the kidneys appeared normal at E12.5 (Fig. 3D,E), decreased metanephric mesenchyme development was evident by E15 (data not shown). This defect was clearly obvious at E18.5 (Fig. 3F,G) and P1, where there were markedly decreased numbers of renal vesicles, and comma- and S-shaped bodies (Fig. 3H,I). The few glomeruli that were seen in the mutant mice were hypoplastic and dysplastic. Mutant pups died within a few hours of birth, presumably due to lack of filtration through the hypoplastic and dysplastic nephrons. Lotus Tetragonolobus Lectin (LTL)-positive proximal tubules were greatly reduced in mutants although they were evident and abundant in wild-type controls at E18.5 (Fig. 3J,K). There was 40% less proliferation of Six2-positive cells as defined by pHH3 staining cells in the metanephric mesenchyme of Six2-cre:Cdc42$^{flox/flox}$ kidneys at E15.5 when compared to Cdc42$^{flox/flox}$ kidneys (Fig. 3L–N) and there were no differences in apoptosis between the two genotypes (data not shown). Thus, removing Cdc42 in the metanephric mesenchyme resulted in severe hypoplasia and dysplasia of the developing renal vesicles and a profound proliferation defect.

Cdc42 is required for normal polarization and differentiation of the ureteric bud

One of the features of the kidneys of the Hoxb7-cre:Cdc42$^{flox/flox}$ mice was obstruction of the tubular lumens (Fig. 1), which suggested polarity defects in the tubular epithelial cells. As a major function of Cdc42 is to regulate epithelial polarity, we defined whether there were abnormalities in expression of the highly conserved polarity proteins that form the Par complex found in the apical domain of polarized epithelial cells. To do this, we performed immunostaining of two key components of the complex, Par3 and atypical protein kinase C (aPKC) in Hoxb7-cre:Cdc42$^{flox/flox}$ mice. There was decreased apical staining of aPKC and Par3 in all cells derived from the ureteric bud (E-cadherin, cytokeratin-double positive epithelia) in Hoxb7-cre:Cdc42$^{flox/flox}$ mice at E15.5 (Fig. 4A–D) and E18.5 (Fig. S1A–D), suggesting that there is a polarity defect in the developing ureteric bud that persists over time. Consistent with these apical polarity abnormalities, there was markedly decreased expression of the tight junction protein ZO-1 (also known as TJP1) in the Hoxb7-cre:Cdc42$^{flox/flox}$ mice (Fig. S1E,F). The cells within the developing ureteric bud of the Hoxb7-cre:Cdc42$^{flox/flox}$ mice also had severe defects of terminal differentiation as they did not express the apical water

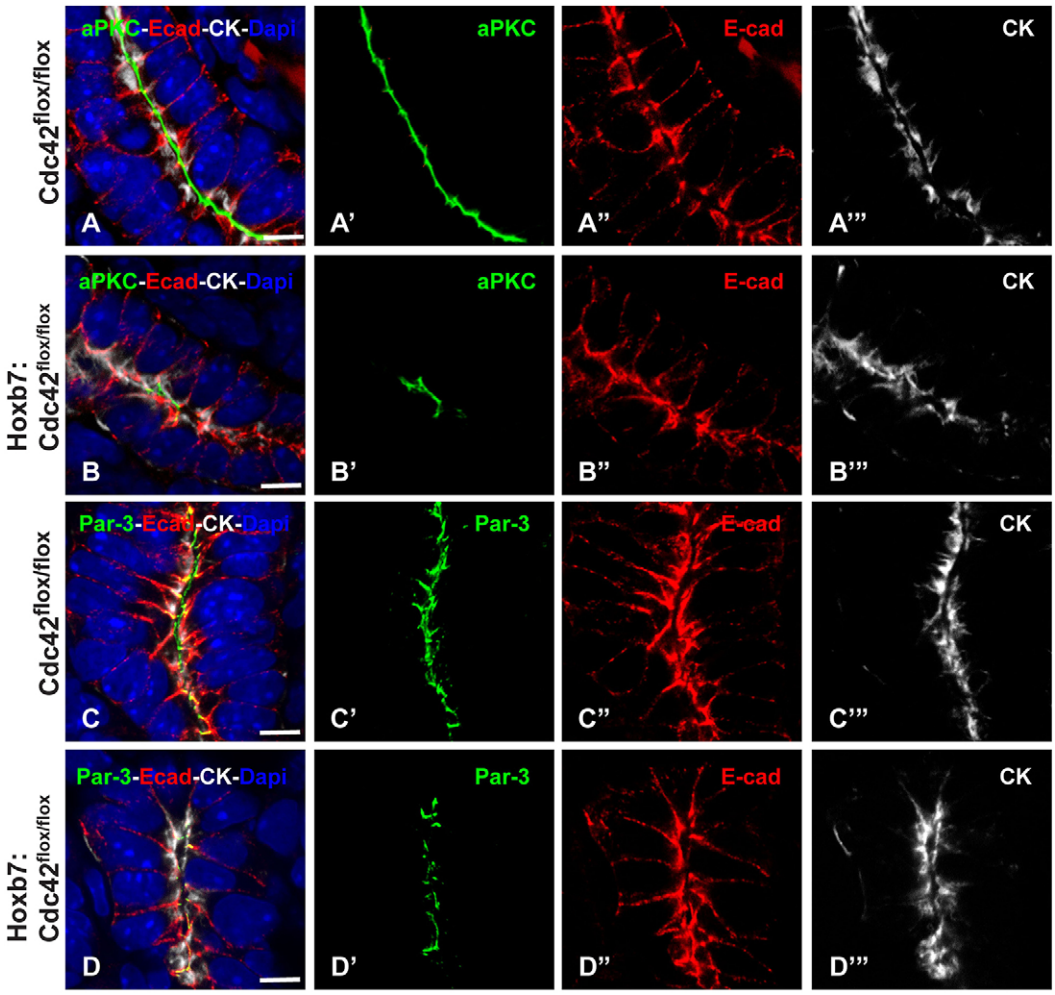

Fig. 4. Localization of apical proteins in the collecting ducts of wild-type and Cdc42 mutant kidneys at E15.5. Immunostaining of E15.5 Cdc42$^{flox/flox}$ (A,A′,A″,C,C′,C″) and Hoxb7-cre:Cdc42$^{flox/flox}$ (B,B′,B″,D,D′,D″) kidneys stained with antibodies to aPKC (green in A,A′,B,B′), Par3 (green in C,C′,D,D′), E-cadherin (red in A″,B″,C″ and D″) and cytokeratin (CK) (white in in A‴,B‴,C‴ and D‴). A,B,C and D are merged panels, with the individual channels being shown in the right-hand panels. All sections have been stained with DAPI (blue in A,B,C,D) to show the nuclei. Scale bars: 20 µm.

Journal of Cell Science (2015) 128, 4293-4305 doi:10.1242/jcs.164509

channel aquaporin-2 (Aqp2), whereas the Cdc42$^{flox/flox}$ mice did (Fig. S1E,F). To verify these terminal differentiation defects of the collecting duct were generalized, we investigated whether there was an altered expression level of the vacuolar-type H ATPase, which is expressed exclusively in the intercalated cells of the collecting duct. This protein was not detectable in the Hoxb7-cre:Cdc42$^{flox/flox}$ mice (Fig. S2A,B). Finally, we also measured the number of cilia present in the Hoxb7-cre:Cdc42$^{flox/flox}$ mice as Cdc42 has been shown to be required for cilia production (Zuo et al., 2011). There were 50% fewer cilia in Hoxb7-cre:Cdc42$^{flox/flox}$ mice compared to Cdc42$^{flox/flox}$ mice (Fig. S2C–E). Taken together, these data indicate that the polarized epithelial cells in the ureteric bud of the Hoxb7-cre:Cdc42$^{flox/flox}$ mice have a profound polarity and terminal differentiation defect, which is associated with decreased primary cilia. These cellular abnormalities likely cause intraluminal tubular obstruction that subsequently results in dilated tubules and obstruction of the kidney.

Defects in metanephric mesenchyme epithelial cell polarity results in abnormal renal vesicle formation

During nephrogenesis, mesenchymal nephron progenitors undergo compaction to form a pretubular aggregate of cells that subsequently form a polarized sphere of epithelia called the renal vesicle, which contains a central lumen. In pretubular aggregates, neural cell adhesion molecule (NCAM, also known as NCAM1) marks the plasma membrane, but becomes restricted to basolateral membranes as a renal vesicle lumen is formed. Pretubular aggregates have little aPKC, and Par-3 is found in dispersed short segments of plasma membrane, called ‘pre-apical domains’ (Yang et al., 2013). As the renal vesicle lumen forms, both aPKC and Par3 become abundant at the apical surface, with Par-3 becoming redistributed to apical and lateral junctions shortly thereafter (Yang et al., 2013). We found that whereas Six2-cre:Cdc42$^{flox/flox}$ kidneys do form NCAM-positive pre-tubular aggregates, these structures do not progress to a structure with a patent lumen by E15.5 (Fig. 5) and E18.5 (Fig. S3). aPKC is greatly reduced or absent from many cells, whereas NCAM remains relatively uniform in its plasma membrane localization. Similar to what is observed for aPKC, many structures at this stage lack Par-3 or contain only small foci of Par-3. As demonstrated previously (Reginensi et al., 2013), deletion of Cdc42 in Six2-positive cells resulted in a marginal reduction in total YAP (also known as YAP1) expression in the metanephric mesenchyme (Fig. S4A,B, arrow). The localization of the phosphorylated form of YAP, however, remained unchanged (Fig. S4C,D). Thus, Cdc42 is needed for the timely initiation of lumen formation during renal vesicle formation and it is associated with reduced YAP expression.

We also examined the next stage of nephrogenesis, when the renal vesicle elongates into a primordial tubule called the S-shaped

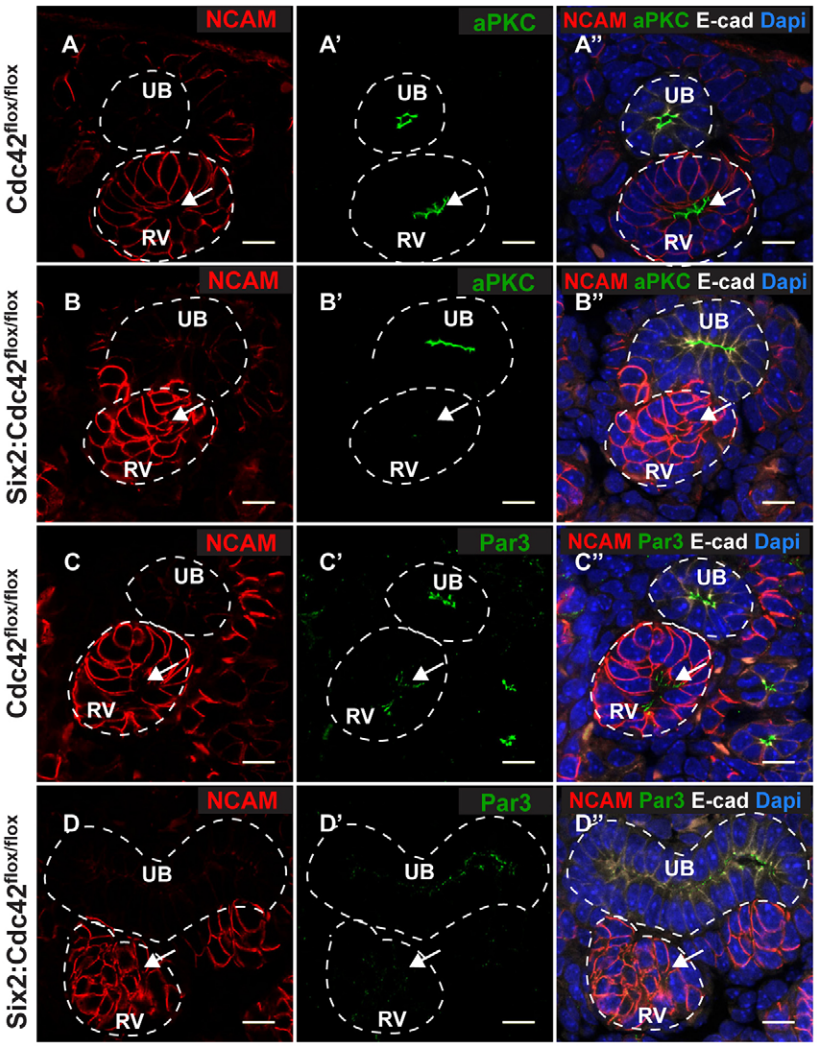

Fig. 5. Cdc42 is essential for timely lumen formation in developing nephrons. Immunostaining of E15.5 kidneys from Cdc42$^{flox/flox}$ (A–A″; C–C″) and Six2-cre:Cdc42$^{flox/flox}$ (B–B″,D–D″) with NCAM (red), aPKC or Par3 (green), E-cadherin (white) and DAPI (blue) as indicated. Controls show luminal clearing of nuclei with apical aPKC, basolateral NCAM and apical-lateral Par3. In contrast, mutants have no evidence of a central clearing of nuclei, display relatively uniform NCAM with little or no aPKC. Mutants also have reduced Par3, with some mutant pretubular aggregate or renal vesicle structures showing none or only small foci of Par3. Results are representative of sections from at least two mice. Similar results were obtained at E18.5 (Fig. S2). Arrows highlight the renal vesicle. RV, renal vesicle; PA, pretubular aggregate; UB, ureteric bud. Ureteric buds and renal vesicles or pretubular aggregates are outlined by a white dotted line. Scale bars: 10 µm.

Journal of Cell Science (2015) 128, 4293-4305 doi:10.1242/jcs.164509

body. In the Cdc42$^{flox/flox}$ kidneys, the elongated S-shaped tubule fuses with the tubule of the ureteric bud and forms a continuous lumen throughout the S-shaped body and ureteric bud at this stage. By contrast, in Six2-cre:Cdc42$^{flox/flox}$ kidneys there is evidence of lumen formation, but the lumens are short and discontinuous despite the apparent fusion of the S-shaped body to the ureteric bud (Fig. 6). The lumens of mutants remain discontinuous even in the later stages of the formation of the S-shaped body, suggesting it is not simply a delay in their ability to inter-connect. From these studies, we conclude that Cdc42 is required not only for timely lumen initiation, but also for continuous lumen formation during kidney morphogenesis.

Collecting duct cells lacking Cdc42 are unable to form tubules and have polarity defects

Our *in vivo* findings suggested that deleting Cdc42 resulted in severe abnormalities in tubulogenesis in both the metanephric mesenchyme and the ureteric bud due at least in part to polarity defects. To determine the mechanism of this deficiency, we isolated collecting duct cells from Cdc42$^{flox/flox}$ mice and deleted Cdc42 *in vitro* using adenoviral-mediated delivery of a plasmid encoding Cre recombinase. We completed serial dilutions on cell populations and identified cells that did not express Cdc42 by immunoblotting (Fig. 7A). We initially performed experiments on at least three different populations to show that the results obtained were not due to clonal selection (data not shown). When Cdc42$^{flox/flox}$ collecting duct cells were placed in 3D collagen-I or matrigel gels, they were unable to form tubules and few cells were observed under these conditions (Fig. 7B,C). Mechanistically, collecting duct cells need to be able to adhere, spread and migrate through extracellular matrix to form tubules. We therefore defined which of these processes were defective in the Cdc42$^{-/-}$ collecting duct cells. We identified a severe adhesion defect in the Cdc42$^{-/-}$ collecting duct cells on collagen I, laminin-111 (data not shown) and -511 (data not shown) and fibronectin (Fig. 7F), although the cells had normal expression of integrin β1, α1, α2, α3, α5 and α6 subunits (data not shown). Thus, deleting Cdc42 altered cell adhesion of collecting duct cells on multiple extracellular matrix (ECM) components, suggesting this adhesion defect was not integrin specific. Consistent with the adhesion defects, these cells had a profound haptotactic migration defect on collagen 1, laminin-111 (data not shown) and -511 (data not shown) and fibronectin (Fig. 7G). They also had a major spreading defect on collagen 1 (Fig. 7D,E), laminin-111 and -511 and fibronectin (data not shown). Owing to the small number of cells seen in the Cdc42$^{-/-}$ collecting duct cell tubulogenesis assay, we performed proliferation assays of these cells on multiple ECMs including collagen 1 and fibronectin under low-serum conditions. In agreement with the results seen *in vivo* and in the *in vitro* 3D assays, there was a marked decrease in Cdc42$^{-/-}$ collecting duct cell proliferation that was independent of the ECM substrate (Fig. 7H). Thus, Cdc42 deletion from collecting duct cells results in a severe

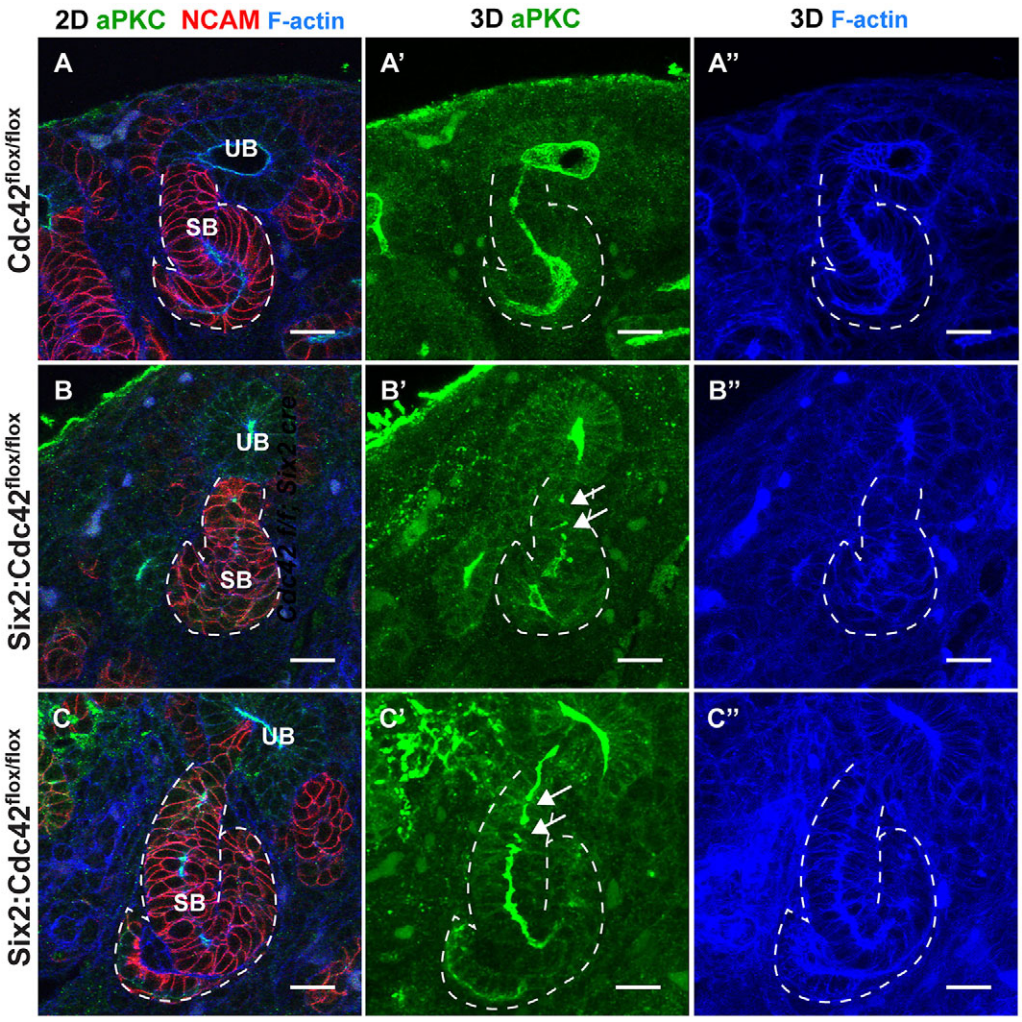

Fig. 6. Cdc42 is required for continuous lumen formation in nephron tubules. Shown are 2D images and 3D reconstructions from confocal *z*-stacks of E15.5 kidneys immunostained with anti-aPKC antibody (green), F-actin (phalloidin, blue) and anti-NCAM (red) antibody as indicated. aPKC marks the apical surface, thereby demarcating the lumen. NCAM delineates basolateral cell membranes of developing nephron tubules. The S-shaped body stage of nephron tubulogenesis is shown in Cdc42$^{flox/flox}$ (A–A″) and Six2-cre:Cdc42$^{flox/flox}$ (B–C″) mice. Images from A and B show S-shaped bodies (SB) at a similar stage, highlighting the discontinuous S-shaped body lumen in mutants (arrows). Images from C show a late S-shaped nephron, illustrating that the discontinuous lumens persist in mutants. Results are representative of sections from at least two mice. Abbreviations: SB, S-shaped body; UB, ureteric bud. The S-shaped body is outlined by a white dotted line. Scale bars: 10 µm.

Journal of Cell Science (2015) 128, 4293-4305 doi:10.1242/jcs.164509

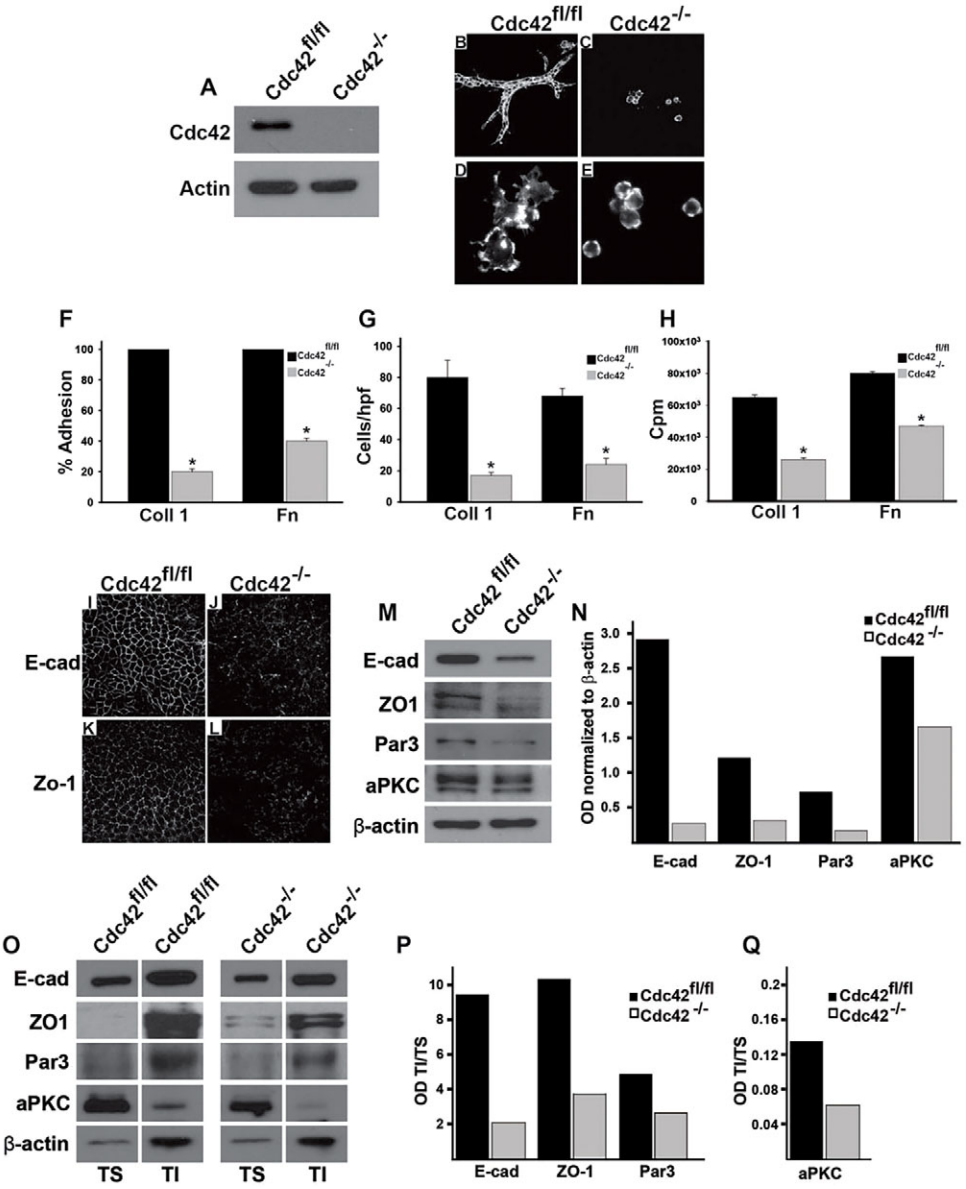

Fig. 7. Deleting Cdc42 from collecting duct cells results in abnormal tubulogenesis, adhesion, migration, proliferation and polarity defects. (A) Immunoblotting was performed on Cdc42$^{flox/flox}$ and Cdc42$^{-/-}$ cell extracts to verify Cdc42 deletion. (B,C) Cdc42$^{flox/flox}$ and Cdc42$^{-/-}$ collecting duct cells were placed into 3D collagen and Matrigel gels and allowed to undergo tubulogenesis over 7 days in the presence of 5% FBS. They were stained with Rhodamine–phalloidin and visualized by confocal microscopy. (D,E) Cdc42$^{flox/flox}$ and Cdc42$^{-/-}$ collecting duct cells were plated on collagen I and allowed to spread for 1 h, after which they were stained with Rhodamine–phalloidin. (F) Cdc42$^{flox/flox}$ and Cdc42$^{-/-}$ collecting duct cells populations were allowed to adhere to collagen I and fibronectin (10 µg/ml) and cell adhesion was evaluated 1 h after plating. (G) Cdc42$^{flox/flox}$ and Cdc42$^{-/-}$ collecting duct cells were plated on Transwells coated with collagen I (10 µg/ml) or fibronectin (10 µg/ml) and migration was evaluated after 4 h. This was quantified and expressed as the number of cells per high-power field (cells/hpf). (H) Cdc42$^{flox/flox}$ and Cdc42$^{-/-}$ collecting duct cells were plated on collagen I. After 24 h, cells were treated with 3H-thymidine and incubated for a further 24 h. 3H-thymidine incorporation was then determined and expressed as counts per minute (cpm) as described in the Materials and Methods. In F–H, values are mean±s.d. from three experiments performed in triplicate. *P<0.01 for the difference between Cdc42$^{flox/flox}$ and Cdc42$^{-/-}$ collecting duct cells (Student's t-test). (I–L) Cdc42$^{flox/flox}$ and Cdc42$^{-/-}$ collecting duct cells were grown to confluence on Transwell inserts and immunostained for ZO-1 and E-cadherin. (M,N) Equal amounts of whole cell lysate from Cdc42$^{flox/flox}$ and Cdc42$^{-/-}$ collecting duct cells were electrophoresed and immunoblotted for E-cadherin, ZO-1, Par3, aPKC and β-actin. The intensities of a single blot were measured and shown on a graph (N), which is representative of at least three similar experiments. (O–Q) Equal amounts of Triton-soluble (TS) and -insoluble (TI) fractions from Cdc42$^{flox/flox}$ and Cdc42$^{-/-}$ collecting duct cells were analyzed by western blotting for E-cadherin, ZO-1, Par3, aPKC and β-actin. The intensities of a single blot were measured and shown graphically (P,Q). This is representative of at least three similar experiments.

collecting duct cell tubulogenesis defect due to decreased adhesion, spreading, migration and proliferation.

Mechanistically, Cdc42 regulates multiple cellular processes, including polarization, actin cytoskeletal organization and cell signaling. Based on our *in vivo* and *in vitro* data, we initially investigated whether the Cdc42$^{-/-}$ collecting duct cells had a polarization defect by growing them on Transwell inserts and performing immunostaining for the adherens junction protein E-cadherin, and the tight junction protein ZO-1. Much less of both these proteins localized to the cell–cell junctions of the Cdc42$^{-/-}$ collecting duct cells when compared to Cdc42$^{fl/fl}$ collecting duct cells (Fig. 7I–L). We next employed biochemical techniques to determine

Journal of Cell Science (2015) 128, 4293-4305 doi:10.1242/jcs.164509

whether there was decreased expression or mislocalization of E-cadherin, ZO-1 and the apical proteins Par3 and aPKC in the $Cdc42^{-/-}$ collecting duct cells. There was marked decrease of E-cadherin, ZO-1 and Par3 and a moderate decrease of aPKC in the $Cdc42^{-/-}$ collecting duct cells (Fig. 7M,N). When we analyzed the relative amounts of these proteins in Triton-soluble and -insoluble cell fractions, there was less E-cadherin, ZO-1, aPKC and Par3 in the Triton-insoluble (membranous) fraction of $Cdc42^{-/-}$ collecting duct cell lysates relative to $Cdc42^{fl/fl}$ (control) cell lysates (Fig. 7O–Q). Taken together, these data demonstrate a polarity defect in $Cdc42^{-/-}$ collecting duct cells, which is consistent with our *in vivo* findings.

$Cdc42^{-/-}$ regulates the actin cytoskeleton in the collecting system of the kidney

The severe adhesion, migration and spreading defect manifested by the $Cdc42^{-/-}$ collecting duct cells suggested they have abnormal integrin-dependent signaling. When we investigated this possibility, no differences between $Cdc42^{f/f}$ and $Cdc42^{-/-}$ collecting duct cells were found when we assessed activation of well recognized signaling proteins such as those of the Akt or ERK family that act downstream of integrins using re-plating assays on collagen 1 or laminin-111 and -511 (data not shown). Cdc42 has also been reported to be a key regulator of cytoskeletal proteins, such as N-Wasp, which activates the Arp2/3 complex, and ezrin, which binds N-Wasp (Albiges-Rizo et al., 2009). When we defined how Cdc42 regulated the activation of these proteins in response to glial-derived neurotropic factor (GDNF), a principal growth factor responsible for ureteric bud branching morphogenesis, phosphorylation of both these proteins was severely decreased in $Cdc42^{-/-}$ compared to $Cdc42^{fl/fl}$ collecting duct cells, despite the same amount of activation of the Ret receptor (Fig. 8A). These data suggest that the severe adhesion, spreading and migration defects observed in the $Cdc42^{-/-}$ collecting duct cells, are due at least in part to the requirement of Cdc42 for N-Wasp and ezrin activation, and that this signaling defect is not due to decreased Ret activation.

We next examined whether an actin cytoskeleton defect was present *in vivo* by staining the developing ureteric bud at E15.5 with Rhodamine–phalloidin. Interestingly there was no obvious structural abnormality in the subapical distribution of actin in the Hoxb7-cre:$Cdc42^{flox/flox}$ mice (Fig. 8B,C). The subapical actin also appeared normal in distribution in the Six2-cre:$Cdc42^{flox/flox}$ mice except in the areas in which there was no discernible lumen (Fig. 6). As a lack of obvious structural defects does not necessarily indicate normal actin cytoskeleton function, we examined the distribution of ezrin. In $Cdc42^{flox/flox}$ mice ezrin staining was clearly expressed in the apex of the lumen of the ureteric bud; however, this staining was decreased and diffuse at the apical surface of collecting ducts in the Hoxb7-cre:$Cdc42^{flox/flox}$ mice (Fig. 8D,E), which is consistent with our *in vitro* data. Taken together, these data demonstrate that Cdc42 is required for apical actin cytoskeletal function in developing collecting ducts, and for N-Wasp and ezrin signaling in collecting duct cells *in vitro*.

DISCUSSION

Cdc42 has diverse cellular functions and plays a role in development of many organs. We show that the absence of Cdc42 in the ureteric bud causes severe branching abnormalities as well as profound polarity and cytoskeletal defects that cause malformed and obstructed tubular lumens. Similarly, deleting Cdc42 from the developing metanephric mesenchyme produces severe abnormalities in epithelial polarity and lumen formation resulting in failed renal vesicle and S-shaped body establishment. We confirmed the requirement for Cdc42 for tubule formation *in vitro* by utilizing Cdc42-null collecting duct cells, which also showed severe adhesion, migration, proliferation, polarization and cytoskeletal defects. Thus, we conclude that the principal role of Cdc42 in ureteric bud and metanephric mesenchyme development is to regulate epithelial cell polarity and actin cytoskeleton function.

It has previously been shown that deletion of Cdc42 in the distal tubule of the kidney using Ksp-cre induced fatal kidney failure; however, the few surviving mice developed cystogenesis associated with decreased ciliogenesis and interstitial fibrosis (Choi et al., 2013). Most of the characterization of these mice was performed within the cysts where increased cell proliferation and apoptosis associated with increased MAPK pathway activation was noted. No epithelial cell polarization defects were observed, as measured by E-cadherin or gp135 (also known as CNTN1) localization. The discrepancies between this and our studies could be attributed to the fact that Hoxb7-cre deletes Cdc42 at the initiation of ureteric bud branching morphogenesis in the newly forming bud tips at E10.5 (Yu et al., 2002). In contrast, Ksp-cre deletes at E12.5 in the stalk region of the ureteric bud, and from E15.5 onward, in more distal segments of the nephron (Karner et al., 2009; Shao et al., 2002). It is not clear whether the cysts observed in the Ksp-cre mutants are in the collecting duct or the distal tubule. It is interesting to note that similar to Choi et al. (2013), we did observe a decrease in cilia number in mutant collecting ducts. This cellular phenotype was not as penetrant as the defects in polarity and differentiation, suggesting that it might be a secondary manifestation of Cdc42 deletion.

Our morphological results of the Six2-cre:$Cdc42^{flox/flox}$ in the developing metanephric mesenchyme are very similar to those reported by Reginensi and colleagues (2013), in that the kidneys were severely hypoplastic with almost no functional nephrons. They concluded that the principal mechanism whereby Cdc42 regulated metanephric mesenchyme development was by altering the cytoskeleton through an N-WASP-dependent mechanism that altered the nuclear localization of YAP. Furthermore, they did not comment on a major proliferation or polarity defect and they reported no changes in Par3 or aPKC localization. Indeed, we did find that deletion of Cdc42 in Six2-positive cells resulted in a marginal reduction in total YAP expression in the metanephric mesenchyme (Fig. S4A,B, arrow), although the expression of the phosphorylated form of YAP appeared unchanged (Fig. S4C,D). Our study identified several other major cellular defects, including abnormalities in epithelial cell polarity and proliferation, tubule lumen formation, and actin cytoskeletal function. We postulate these are the primary causes of the defects in terminal differentiation of both the nephron and the collecting duct epithelia. Our study is consistent with the findings in other branching organs, such as the pancreas (Kesavan et al., 2009) and lung (Wan et al., 2013), where epithelial deletion of Cdc42 has been shown to be required for branching, epithelial cell proliferation, tubule formation, normal apical polarity and actin cytoskeleton formation as well as terminal differentiation and cell fate specification. In addition, hepatocytes from Cdc42-null mice are unable to proliferate in response to hepatectomy (Yuan et al., 2009) and deleting Cdc42 from the colon results in a mild defect in apical junction orientation and impaired intestinal epithelium polarity (Melendez et al., 2013), clearly demonstrating a role for Cdc42 in epithelial cell proliferation and polarity.

Our observations in both the ureteric bud and metanephric mesenchyme are very similar to those demonstrated in pancreatic duct formation, where Cdc42 plays a cell-autonomous role in microlumen formation, in generation of apical polarity and in tight junction formation (Kesavan et al., 2009). Therefore, we propose

Journal of Cell Science (2015) 128, 4293-4305 doi:10.1242/jcs.164509

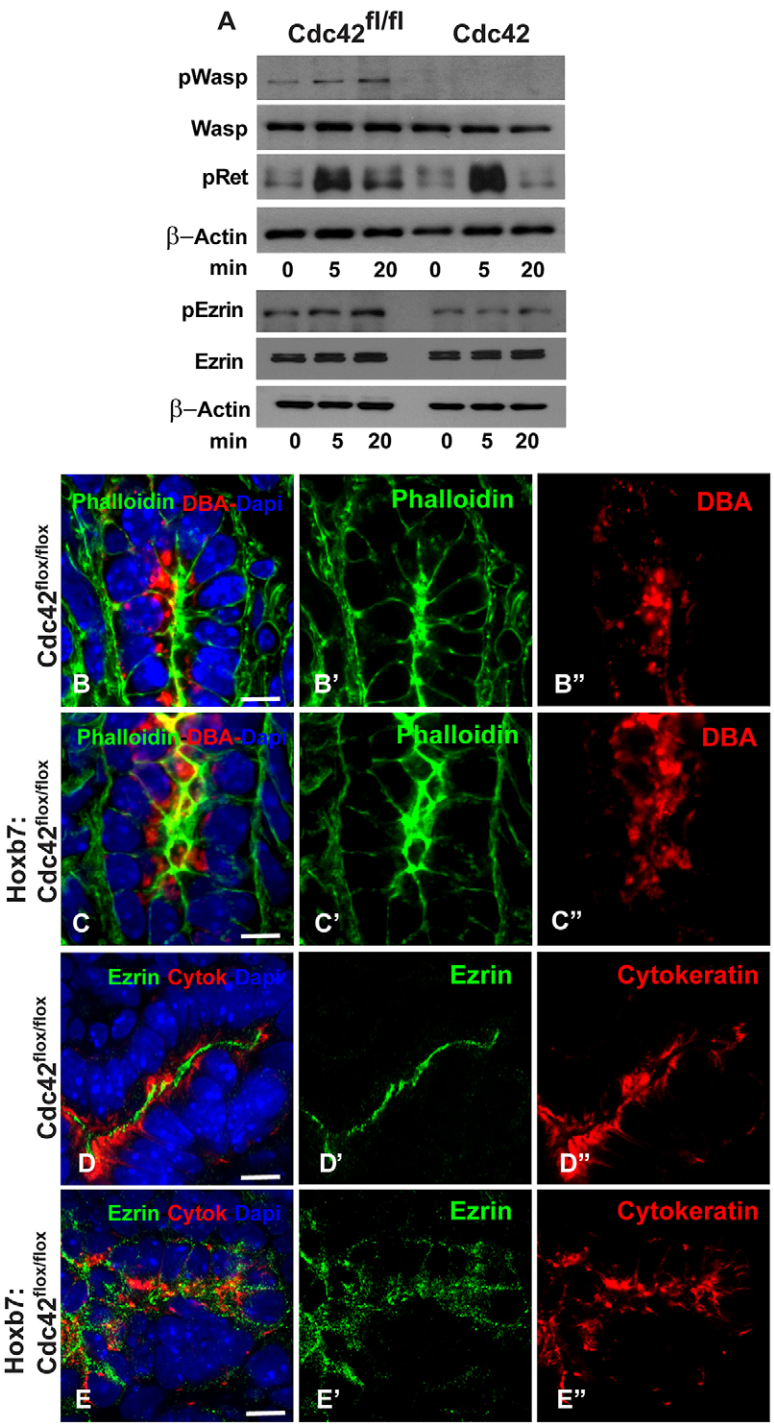

Fig. 8. Deleting Cdc42 from collecting ducts results in cytoskeletal abnormalities. (A) Cdc42$^{flox/flox}$ and Cdc42$^{-/-}$ collecting duct cells were allowed to adhere to collagen I for 1 h, after which they were treated with GDNF for 5 and 20 min. The cells were then lysed and analyzed by western blotting for levels of phosphorylated N-Wasp (pWasp), N-Wasp, phosphorylated Ret (pRet), phosphorylated ezrin (pEzrin), ezrin and β-actin. (B–E) Immunostaining of E15.5 Cdc42$^{flox/flox}$ (B,B′,B″,D,D′,D″) and Hoxb7-cre:Cdc42$^{flox/flox}$ (C,C′,C″,E,E′,E″) kidney sections with phalloidin (green in B–C″), the collecting duct marker DBA (red in B–C″), the nuclear marker DAPI (blue in B,C,D and E), the sub-apical marker ezrin (green in D–E″) and the collecting duct marker cytokeratin (red in D–E″). B,C,D and E represent merged images; B′ and C′ are single images for phalloidin; B″ and C″ are single images for DBA; D′ and E′ are single images for ezrin; and D″ and E″ are single images for cytokeratin. Scale bars: 20 µm.

that the tubular lumen and cell differentiation lesions in the Hoxb7-cre:Cdc42$^{flox/flox}$ and Six2-cre:Cdc42$^{flox/flox}$ mice are primarily caused by abnormalities in epithelial cell polarity due to defects in Cdc42-dependent aPKC activation through Par6 (Goldstein and Macara, 2007) and abnormal apical actin cytoskeletal function caused by abnormal N-Wasp activation as described in other systems (Rohatgi et al., 2000, 1999). The Cdc42 Six2-cre mice have a phenotype that is similar to mice lacking afadin: both are defined by their polarity defects and discontinuous lumen formation as evidenced by a decrease in Par3 staining in the pretubular aggregates and/or renal vesicles, and the absence of a discrete lumen at the renal vesicle stage (Yang et al., 2013). The Six2-cre:Cdc42$^{flox/flox}$ mutants do not pass through a true renal vesicle stage and small discontinuous lumens develop in S-shaped bodies resulting in a persistent defect in luminal continuity. There are increased levels of both Par3 and aPKC in S-shaped bodies of Cdc42 Six2-cre mutants compared with earlier stages. The mechanisms responsible for this ‘recovery’ of the localization of Par complex components are unknown, but it is likely that partially redundant signaling pathways compensate for this process in the absence of Cdc42. Similar to the Cdc42 mutants, afadin mutants also have defects in the actin cytoskeleton as they are unable to recruit the actin subapical ring to form apical surfaces. In addition, afadin mutants fail to form Par complexes. Taken together, these results suggest that Cdc42 and

Journal of Cell Science (2015) 128, 4293-4305 doi:10.1242/jcs.164509

afadin act in a similar pathway to promote polarization and lumen formation. Based on *in vitro* data from others (Kawakatsu et al., 2002; Kurita et al., 2013; Mandai et al., 2013; Nakanishi and Takai, 2004), we speculate that afadin acts upstream of Cdc42 in the signaling pathway; however, this still needs to be verified.

We used Cdc42$^{-/-}$ collecting duct cells to demonstrate that Cdc42 is required for *in vitro* 3D tubulogenesis as well as collecting duct cell adhesion, migration and proliferation on all extracellular matrices. Similar to our *in vivo* findings, these cells also have a major abnormality in epithelial cell polarity with respect to formation of adherens and tight junctions as well as the Par3–Par6–aPKC complex. Our results are similar to those demonstrating a role for Cdc42 in polarized mammary epithelial cell migration and branching, where Cdc42 was either overexpressed or knocked down *in vitro* (Duan et al., 2010), and overexpressed in the mouse mammary gland *in vivo* (Bray et al., 2013). In the kidney tubular epithelium, the functional characteristics of Cdc42 have been explored in the well-characterized polarized MDCK cells. Utilizing overexpression and knockdown techniques, Cdc42 has been shown to be required for lumen formation of tubules because it mediates exocytosis of large intracellular vacuoles that become the lumen and it also binds to the Par3–Par6–aPKC complex, which regulates tight junction formation and epithelial cell polarity (Martin-Belmonte et al., 2007, 2008; Martin-Belmonte and Mostov, 2007; Rodriguez-Fraticelli et al., 2010). In addition Cdc42 has been shown to play a role in localizing the exocyst to the primary cilium of MDCK cells (Zhang et al., 2001; Zuo et al., 2011). The effects of deleting Cdc42 on MDCK cell tubulogenesis are much less severe than those seen in the Cdc42$^{-/-}$ collecting duct cells, which never progress to the cyst stage in 3D culture. These data suggest very distinct roles for Cdc42 in tubulogenesis and lumen formation in collecting duct and MDCK cells, and that Cdc42 plays multiple roles in tubule formation in different cell types.

We demonstrate that the principal signaling defect observed in Cdc42$^{-/-}$ collecting duct cells is their inability to activate N-Wasp and ezrin in response to growth factors. There was also a major defect of apical ezrin expression and localization in collecting ducts *in vivo*. Taken together, these data suggest that local recruitment of activated Cdc42 and its downstream effector, N-Wasp, can trigger actin polymerization in the apical domain of the epithelial cell (Castellano et al., 1999; Nakamura et al., 2000). This is consistent with the well-defined role of Cdc42 in localizing the Par3–Par6–aPKC complex to the apical part of a polarized epithelial cell (Joberty et al., 2000; Welchman et al., 2007).

In conclusion, we and others have shown that Cdc42 is required for normal tubulogenesis in ureteric bud and metanephric mesenchyme development of the kidney (Choi et al., 2013; Reginensi et al., 2013). Although the morphological observations are similar in all these studies, the mechanisms proposed differ. We demonstrate both *in vivo* and *in vitro* that the predominant role of Cdc42 in renal tubulogenesis, as in other branching organs like the lung (Wan et al., 2013) and the pancreas (Kesavan et al., 2009), is to regulate epithelial cell proliferation, polarity and the actin cytoskeleton. Thus, in keeping with its pleiotropic effects, Cdc42 regulates epithelial cell tubulogenesis by multiple mechanisms. This emphasizes the importance of studying its cell autonomous functions in different situations in epithelial cell biology.

MATERIALS AND METHODS

Mice

All experiments were approved by the Vanderbilt University Institutional Animal Use and Care Committee. Cdc42$^{flox/flox}$ mice, which were previously described (Wu et al., 2006), were crossed with the Hoxb7Cre mice (generous gift of Andrew McMahon, Department of Stem Cell Biology and Regenerative Medicine, USC Keck School of Medicine, CA) (Yu et al., 2002) or Six2-cre mice (generous gift of Andrew McMahon) (Kobayashi et al., 2008). Mice were a F4–F6 generation towards the C57/B6 background. Aged-matched littermates Cdc42$^{flox/flox}$ mice were used as controls.

Morphologic and immunofluorescence analysis

For morphological and immunohistochemical analysis, kidneys were removed at different stages of development and fixed in 4% formaldehyde and embedded in paraffin. Paraffin tissue sections were stained with either hematoxylin and eosin or periodic acid Schiff's (PAS) for morphological evaluation by light microscopy.

Immunofluorescence was performed as previously described (Yang et al., 2013). In brief, fixed sections (4% PFA for 2 h) were permeabilized with 0.3% Triton X-100 in PBS (PBST) and blocked with 10% bovine serum albumin (BSA) in PBST. Sections were incubated with primary antibodies overnight (4°C), then with fluorophore-conjugated secondary antibodies and mounted with Vecatshield (Vector Laboratories). Antibodies used were against Par3 (1:150, Millipore, 07-330), aPKCζ (1:400, Santa Cruz Biotechnology, C-20) and phalloidin 647 and 488 (1:200, Invitrogen, 42008A), YAP and phosphorylated YAP (1:500, Cell Signaling 4912, 4911, tyramide amplification), V-ATPase (1:500, Santa Cruz Biotechnology, 20943), cytokeratin (1:500, Sigma-Aldrich, C2562), LTL (1:500, Vector Labs, B1325), NCAM (1:500, no antigen retrieval), E-cadherin (1:300, Invitrogen), DBA (1:500, Vector Labs, B1035), ezrin (1:500, Upstate 07-130), ZO1 (Santa Cruz Biotechnology, 33725), Aqp2 (Sigma-Aldrich A7310), acetylated αtubulin (Cell Signaling, 5335P) and Six2 (Proteintech, 11562-1). Secondary antibodies were purchased from Jackson ImmunoResearch and Alexa-Fluor-conjugated antibodies from Invitrogen.

Cell proliferation *in vivo*

Kidney sections obtained at different embryonic stages were subjected to immunohistochemical analysis using primary antibodies against phosphorylated histone H3 (pHH3, 1:2000, Sigma-Aldrich, tyramide amplification), Six2 (1:500, Proteintech) and cytokeratin (1:500, Sigma-Aldrich). More than 250 Six2- or cytokeratin-positive cells were counted from each kidney at each stage and the percentage of pHH3 co-positive cells were calculated. For each stage and genotype a minimum of four different embryos were analyzed.

Generation of Cdc42$^{-/-}$ cells

Collecting duct cells were isolated from Cdc42$^{fl/fl}$ mice following the methodology described by Husted et al. (1988) and Cdc42 was deleted by infecting the cells with an adenocre virus *in vitro*. Deletion of Cdc42 was verified by immunoblotting for Cdc42. Clonal Cdc42-null cell lines were generated and similarity in their behavior was verified.

Tubulogenesis assay

Collecting duct cells were grown in collagen or matrigel gels as previously described (Chen et al., 2004). Collecting duct cells (5×10^3) were seeded into the gels, which were overlaid with 100 µl of medium and allowed to grow for 5 to 7 days. The gels were stained with Rhodamine–phalloidin (R415, 1:2000, Molecular Probes) and the tubules were photographed using a Zeiss Axio 510 confocal microscope (400×).

Cell spreading

Cells were plated onto slides coated with collagen I (10 µg/ml) for 2 h after which they were fixed, permeabilized, exposed to Rhodamine–phalloidin (1:5000) and visualized under a fluorescence microscope.

Cell adhesion and migration assays

Cell adhesion and migration assays on different ECM components were performed as described previously (Chen et al., 2004). Four independent experiments were performed in triplicate.

Cell proliferation

Proliferation assays were performed as previously described (Chen et al., 2004). Briefly, 5×10^3cells were plated on different ECM components in

96-well plates and maintained in Dulbecco's modified Eagle's medium (DMEM) with 10% fetal bovine serum (FBS). After 12 h, the cells were switched to DMEM (2% FBS) for 24 h and then pulsed with 1 µCi/well [3H]thymidine (PerkinElmer Life Sciences). After another 24 h, the cells were solubilized and radioactivity was measured using a scintillation counter.

Cell polarity

Cells were grown on Transwell inserts consisting of polyvinylpyrolidone-free polycarbonate filters with 0.4 µm pores. After reaching confluency, cells were fixed in 4% formaldehyde and incubated with anti-ZO-1 (1:200; BD Transduction Laboratories) or anti-E-cadherin (1:1000; BD Transduction Laboratories) antibodies followed by the appropriate FITC-conjugated secondary antibody. Chamber slides were mounted and viewed using a confocal microscope.

Immunoblotting

The effect of glial-derived neurotropic factor (GDNF) on collecting duct cells was examined as previously described (Zhang et al., 2009). In brief, cells were trypsinized into serum-free DMEM and then plated on collagen I (10 µg/ml) for 45 min. GDNF (10 ng/ml) was added to the medium and the cells were lysed at different time points following growth factor stimulation.

For analysis on kidney tissues, the cortices or medullas were removed and lysed with T-Per buffer (ThermoScientific). Lysates were clarified by centrifugation, and 30 µg total protein was electrophoresed onto a 10% SDS-PAGE gel and subsequently transferred to PVDF membranes. Membranes were blocked in 5% milk with TBS containing 0.1% Tween 20 and then incubated with the different primary antibodies followed by the appropriate horseradish peroxidase (HRP)-conjugated secondary antibodies.

Immunoreactive bands were identified using enhanced chemiluminescence according to the manufacturer's instructions. Antibodies against Cdc42 (2466, 1:1000), ezrin (3142, 1:1000), phosphorylated ezrin (3144, 1:1000) and phosphorylated Ret (3221, 1:1000) were purchased from Cell Signaling; anti-PKCζ antibody was from Upstate (17264, 1:1000), anti-ParD3A (sc-98509, 1:1000) antibody was from Santa Cruz Biotechnology, antibodies against N-Wasp (wp2001, 1:1000) and phosphorylated N-Wasp (wp2601, 1:1000) were from ECM Biosciences, anti-ZO-1 (33-9100, 1:1000) antibody was from Life Technologies and anti-E-cadherin antibody (610181, 1:2000) was from BD Biosciences

Cell fractionation

Triton-insoluble (actin-rich) and Triton-soluble fractions of collecting duct cells were prepared as described previously (Elias et al., 2014). Briefly, cells were incubated for 5 min with lysis buffer CS (50 mm Tris-HCl, pH 7.4, 1.0% Triton X-100, 5 mm EGTA, and 10 µg/ml protease inhibitor mixture). Cell lysates were centrifuged at 15,600 ***g*** for 5 min at 4°C to sediment the high-density actin-rich fraction. The pellet was suspended in 200 µl of lysis buffer D (0.3% SDS in 20 mm Tris-HCl buffer, pH 7.4, and 10 µg/ml protease inhibitor mixture).

Statistics

The Student's *t*-test was used for comparisons between two groups, and analysis of variance using Sigma Stat software was used for statistical differences between multiple groups. $P<0.05$ was considered statistically significant.

Competing interests

The authors declare no competing or financial interests.

Author contributions

Bertha C. Elias, Amrita Das, Diptiben V. Parekh, Glenda Mernaugh, Rebecca Adams, Zhufeng Yang and Denise K. Marciano performed experiments for the paper. Cord Brakebusch made the floxed Cdc42 mice. Ambra Pozzi, Bertha Elias, Denise K. Marciano, Thomas J. Carroll and Roy Zent wrote the paper.

Funding

This research was funded by VA Merit Reviews [grant numbers 1I01BX002025 to A.P., 1I01BX002196 to R.Z.]; by the National Institutes of Health [grant numbers R01-DK083187 to R.Z., R01-DK075594 to R.Z., R01-DK383069221 to R.Z., R01-DK095761 to A.P., RO1-DK080004 to T.J.C., RO1-DK095057to T.J.C., R01-DK099478 to D.K.M., 5P30DK-079328 to T.J.C.]; and by March of Dimes grants to T.J.C. and D.K.M. Deposited in PMC for release after 12 months.

Supplementary information

Supplementary information available online at
http://jcs.biologists.org/lookup/suppl/doi:10.1242/jcs.164509/-/DC1

References

Albiges-Rizo, C., Destaing, O., Fourcade, B., Planus, E. and Block, M. R. (2009). Actin machinery and mechanosensitivity in invadopodia, podosomes and focal adhesions. *J. Cell Sci.* **122**, 3037-3049.

Bray, K., Gillette, M., Young, J., Loughran, E., Hwang, M., Sears, J. C. and Vargo-Gogola, T. (2013). Cdc42 overexpression induces hyperbranching in the developing mammary gland by enhancing cell migration. *Breast Cancer Res.* **15**, R91.

Carroll, T. J. and Das, A. (2013). Defining the signals that constitute the nephron progenitor niche. *J. Am. Soc. Nephrol.* **24**, 873-876.

Castellano, F., Montcourrier, P., Guillemot, J.-C., Gouin, E., Machesky, L., Cossart, P. and Chavrier, P. (1999). Inducible recruitment of Cdc42 or WASP to a cell-surface receptor triggers actin polymerization and filopodium formation. *Curr. Biol.* **9**, 351-361.

Chen, D., Roberts, R., Pohl, M., Nigam, S., Kreidberg, J., Wang, Z., Heino, J., Ivaska, J., Coffa, S., Harris, R. C. et al. (2004). Differential expression of collagen- and laminin-binding integrins mediates ureteric bud and inner medullary collecting duct cell tubulogenesis. *Am. J. Physiol. Renal Physiol.* **287**, F602-F611.

Choi, S. Y., Chacon-Heszele, M. F., Huang, L., McKenna, S., Wilson, F. P., Zuo, X. and Lipschutz, J. H. (2013). Cdc42 deficiency causes ciliary abnormalities and cystic kidneys. *J. Am. Soc. Nephrol.* **24**, 1435-1450.

Costantini, F. and Kopan, R. (2010). Patterning a complex organ: branching morphogenesis and nephron segmentation in kidney development. *Dev. Cell* **18**, 698-712.

Dressler, G. R. (2006). The cellular basis of kidney development. *Annu. Rev. Cell Dev. Biol.* **22**, 509-529.

Duan, L., Chen, G., Virmani, S., Ying, G., Raja, S. M., Chung, B. M., Rainey, M. A., Dimri, M., Ortega-Cava, C. F., Zhao, X. et al. (2010). Distinct roles for Rho versus Rac/Cdc42 GTPases downstream of Vav2 in regulating mammary epithelial acinar architecture. *J. Biol. Chem.* **285**, 1555-1568.

Elias, B. C., Mathew, S., Srichai, M. B., Palamuttam, R., Bulus, N., Mernaugh, G., Singh, A. B., Sanders, C. R., Harris, R. C., Pozzi, A. et al. (2014). The integrin beta 1 subunit regulates paracellular permeability of kidney proximal tubule cells. *J. Biol. Chem.* **289**, 8532-8544.

Goldstein, B. and Macara, I. G. (2007). The PAR proteins: fundamental players in animal cell polarization. *Dev. Cell* **13**, 609-622.

Husted, R. F., Hayashi, M. and Stokes, J. B. (1988). Characteristics of papillary collecting duct cells in primary culture. *Am. J. Physiol.* **255**, F1160-F1169.

Joberty, G., Petersen, C., Gao, L. and Macara, I. G. (2000). The cell-polarity protein Par6 links Par3 and atypical protein kinase C to Cdc42. *Nat. Cell Biol.* **2**, 531-539.

Karner, C. M., Chirumamilla, R., Aoki, S., Igarashi, P., Wallingford, J. B. and Carroll, T. J. (2009). Wnt9b signaling regulates planar cell polarity and kidney tubule morphogenesis. *Nat. Genet.* **41**, 793-799.

Kawakatsu, T., Shimizu, K., Honda, T., Fukuhara, T., Hoshino, T. and Takai, Y. (2002). Trans-interactions of nectins induce formation of filopodia and Lamellipodia through the respective activation of Cdc42 and Rac small G proteins. *J. Biol. Chem.* **277**, 50749-50755.

Kesavan, G., Sand, F. W., Greiner, T. U., Johansson, J. K., Kobberup, S., Wu, X., Brakebusch, C. and Semb, H. (2009). Cdc42-mediated tubulogenesis controls cell specification. *Cell* **139**, 791-801.

Kim, M., Datta, A., Brakeman, P., Yu, W. and Mostov, K. E. (2007). Polarity proteins PAR6 and aPKC regulate cell death through GSK-3beta in 3D epithelial morphogenesis. *J. Cell Sci.* **120**, 2309-2317.

Kobayashi, A., Valerius, M. T., Mugford, J. W., Carroll, T. J., Self, M., Oliver, G. and McMahon, A. P. (2008). Six2 defines and regulates a multipotent self-renewing nephron progenitor population throughout mammalian kidney development. *Cell Stem Cell* **3**, 169-181.

Kurita, S., Yamada, T., Rikitsu, E., Ikeda, W. and Takai, Y. (2013). Binding between the junctional proteins afadin and PLEKHA7 and implication in the formation of adherens junction in epithelial cells. *J. Biol. Chem.* **288**, 29356-29368.

Mandai, K., Rikitake, Y., Shimono, Y. and Takai, Y. (2013). Afadin/AF-6 and canoe: roles in cell adhesion and beyond. *Prog. Mol. Biol. Transl. Sci.* **116**, 433-454.

Martin-Belmonte, F. and Mostov, K. (2007). Phosphoinositides control epithelial development. *Cell Cycle* **6**, 1957-1961.

Martin-Belmonte, F., Gassama, A., Datta, A., Yu, W., Rescher, U., Gerke, V. and Mostov, K. (2007). PTEN-mediated apical segregation of phosphoinositides controls epithelial morphogenesis through Cdc42. *Cell* **128**, 383-397.

Martin-Belmonte, F., Yu, W., Rodriguez-Fraticelli, A. E., Ewald, A., Werb, Z., Alonso, M. A. and Mostov, K. (2008). Cell-polarity dynamics controls the mechanism of lumen formation in epithelial morphogenesis. *Curr. Biol.* **18**, 507-513.

Melendez, J., Grogg, M. and Zheng, Y. (2011). Signaling role of Cdc42 in regulating mammalian physiology. *J. Biol. Chem.* **286**, 2375-2381.

Melendez, J., Liu, M., Sampson, L., Akunuru, S., Han, X., Vallance, J., Witte, D., Shroyer, N. and Zheng, Y. (2013). Cdc42 coordinates proliferation, polarity, migration, and differentiation of small intestinal epithelial cells in mice. *Gastroenterology* **145**, 808-819.

Nakamura, N., Oshiro, N., Fukata, Y., Amano, M., Fukata, M., Kuroda, S., Matsuura, Y., Leung, T., Lim, L. and Kaibuchi, K. (2000). Phosphorylation of ERM proteins at filopodia induced by Cdc42. *Genes Cells* **5**, 571-581.

Nakanishi, H. and Takai, Y. (2004). Roles of nectins in cell adhesion, migration and polarization. *Biol. Chem.* **385**, 885-892.

Reginensi, A., Scott, R. P., Gregorieff, A., Bagherie-Lachidan, M., Chung, C., Lim, D.-S., Pawson, T., Wrana, J. and McNeill, H. (2013). Yap- and Cdc42-dependent nephrogenesis and morphogenesis during mouse kidney development. *PLoS Genet.* **9**, e1003380.

Rodriguez-Fraticelli, A. E., Vergarajauregui, S., Eastburn, D. J., Datta, A., Alonso, M. A., Mostov, K. and Martin-Belmonte, F. (2010). The Cdc42 GEF Intersectin 2 controls mitotic spindle orientation to form the lumen during epithelial morphogenesis. *J. Cell Biol.* **189**, 725-738.

Rogers, K. K., Jou, T.-S., Guo, W. and Lipschutz, J. H. (2003). The Rho family of small GTPases is involved in epithelial cystogenesis and tubulogenesis. *Kidney Int.* **63**, 1632-1644.

Rohatgi, R., Ma, L., Miki, H., Lopez, M., Kirchhausen, T., Takenawa, T. and Kirschner, M. W. (1999). The interaction between N-WASP and the Arp2/3 complex links Cdc42-dependent signals to actin assembly. *Cell* **97**, 221-231.

Rohatgi, R., Ho, H.-Y. and Kirschner, M. W. (2000). Mechanism of N-WASP activation by CDC42 and phosphatidylinositol 4,5-bisphosphate. *J. Cell Biol.* **150**, 1299-1310.

Shao, X., Somlo, S. and Igarashi, P. (2002). Epithelial-specific Cre/lox recombination in the developing kidney and genitourinary tract. *J. Am. Soc. Nephrol.* **13**, 1837-1846.

Wan, H., Liu, C., Wert, S. E., Xu, W., Liao, Y., Zheng, Y. and Whitsett, J. A. (2013). CDC42 is required for structural patterning of the lung during development. *Dev. Biol.* **374**, 46-57.

Welchman, D. P., Mathies, L. D. and Ahringer, J. (2007). Similar requirements for CDC-42 and the PAR-3/PAR-6/PKC-3 complex in diverse cell types. *Dev. Biol.* **305**, 347-357.

Wu, X., Quondamatteo, F., Lefever, T., Czuchra, A., Meyer, H., Chrostek, A., Paus, R., Langbein, L. and Brakebusch, C. (2006). Cdc42 controls progenitor cell differentiation and beta-catenin turnover in skin. *Genes Dev.* **20**, 571-585.

Yang, Z., Zimmerman, S., Brakeman, P. R., Beaudoin, G. M., III, Reichardt, L. F. and Marciano, D. K. (2013). De novo lumen formation and elongation in the developing nephron: a central role for afadin in apical polarity. *Development* **140**, 1774-1784.

Yu, J., Carroll, T. J. and McMahon, A. P. (2002). Sonic hedgehog regulates proliferation and differentiation of mesenchymal cells in the mouse metanephric kidney. *Development* **129**, 5301-5312.

Yuan, H., Zhang, H., Wu, X., Zhang, Z., Du, D., Zhou, W., Zhou, S., Brakebusch, C. and Chen, Z. (2009). Hepatocyte-specific deletion of Cdc42 results in delayed liver regeneration after partial hepatectomy in mice. *Hepatology* **49**, 240-249.

Zhang, X., Bi, E., Novick, P., Du, L., Kozminski, K. G., Lipschutz, J. H. and Guo, W. (2001). Cdc42 interacts with the exocyst and regulates polarized secretion. *J. Biol. Chem.* **276**, 46745-46750.

Zhang, X., Mernaugh, G., Yang, D.-H., Gewin, L., Srichai, M. B., Harris, R. C., Iturregui, J. M., Nelson, R. D., Kohan, D. E., Abrahamson, D. et al. (2009). beta1 integrin is necessary for ureteric bud branching morphogenesis and maintenance of collecting duct structural integrity. *Development* **136**, 3357-3366.

Zuo, X., Fogelgren, B. and Lipschutz, J. H. (2011). The small GTPase Cdc42 is necessary for primary ciliogenesis in renal tubular epithelial cells. *J. Biol. Chem.* **286**, 22469-22477.

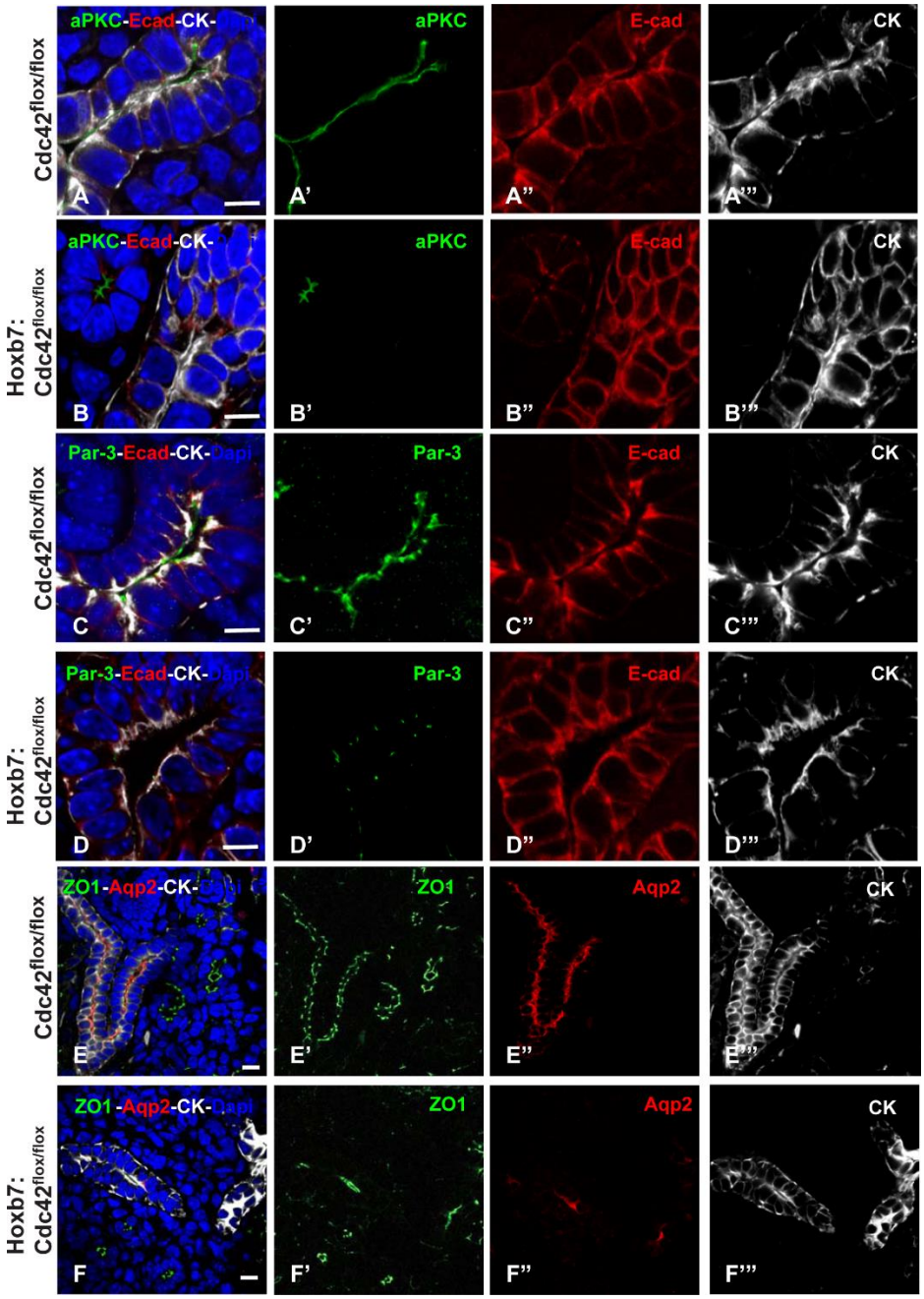

Supplemental Figure 1. Localization of apical proteins in Cdc42$^{flox/flox}$ and Hoxb7-cre;Cdc42$^{flox/flox}$ kidneys at E18.5. Immunostaining of aPKC (green in A and B), Par3 (green in C and D) ZO-1 (green in E and F) and Aqp2 (red in E and F) in Cdc42$^{flox/flox}$ and Hoxb7-cre;Cdc42$^{flox/flox}$ kidneys at E18.5. E-cadherin (red) (A"-D") marks all epithelial structures and cytokeratin (white) (A'"-F'") marks only the collecting duct epithelium in all panels. Scale bars: 20 μm.

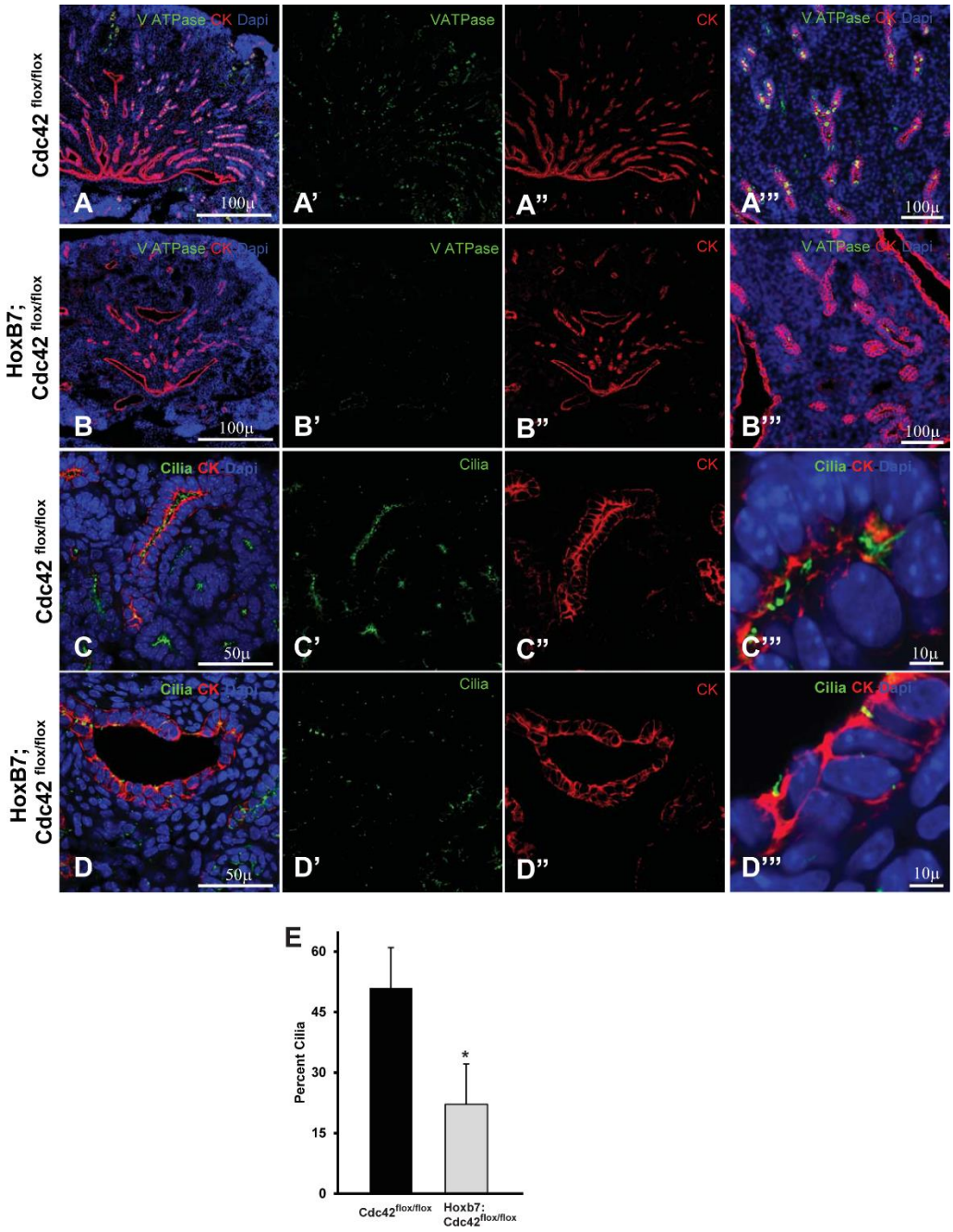

Supplemental Figure 2. E18.5 Cdc42$^{flox/flox}$ (A, C) and Hoxb7-cre;Cdc42$^{flox/flox}$ kidneys (B, D) were analyzed for the expression of VATPase (green in A, A', B, B') and acetylated tubulin (green in C,C', D, D'). The collecting duct structures are marked with the expression of cytokeratin, CK in red (A, A", B, B", C,C", D,D"). Higher magnification of A, B, C, D are shown in A'", B'", C'", D'". The percent of UB cells with cilia are shown in E. Differences between Cdc42$^{flox/flox}$ and the Hoxb7-cre;Cdc42$^{flox/flox}$ mice (*) were significant (P<0.01). The length of the scale bars is marked on the figure.

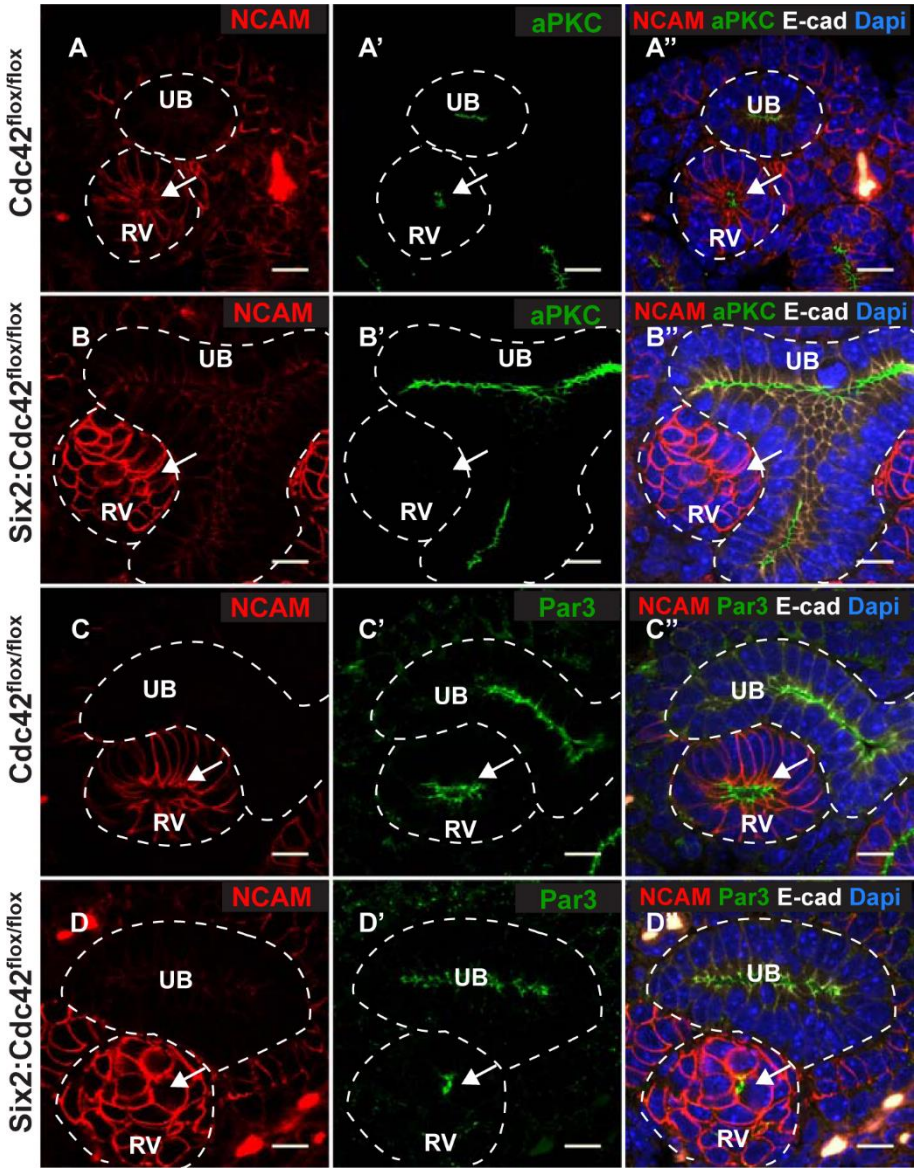

Supplemental Figure 3. Cdc42 is essential for timely lumen formation in developing nephrons at E18.5. Immunostaining of E18.5 kidneys from Cdc42$^{flox/flox}$ (A-A''; C-C'') and Six2-cre:Cdc42$^{flox/flox}$ (B-B'', D-D'') with NCAM (red), aPKC or Par-3 (green), E-cadherin (white), and Dapi (blue) as indicated. The arrows point to the lumens of the renal vesicles. Results are representative of sections from at least 2 mice. Abbreviations: RV, renal vesicle; PA, pretubular aggregate, UB, ureteric bud. UB and RV/PA are outlined by a white dotted line. Scale bars: 10 μm.

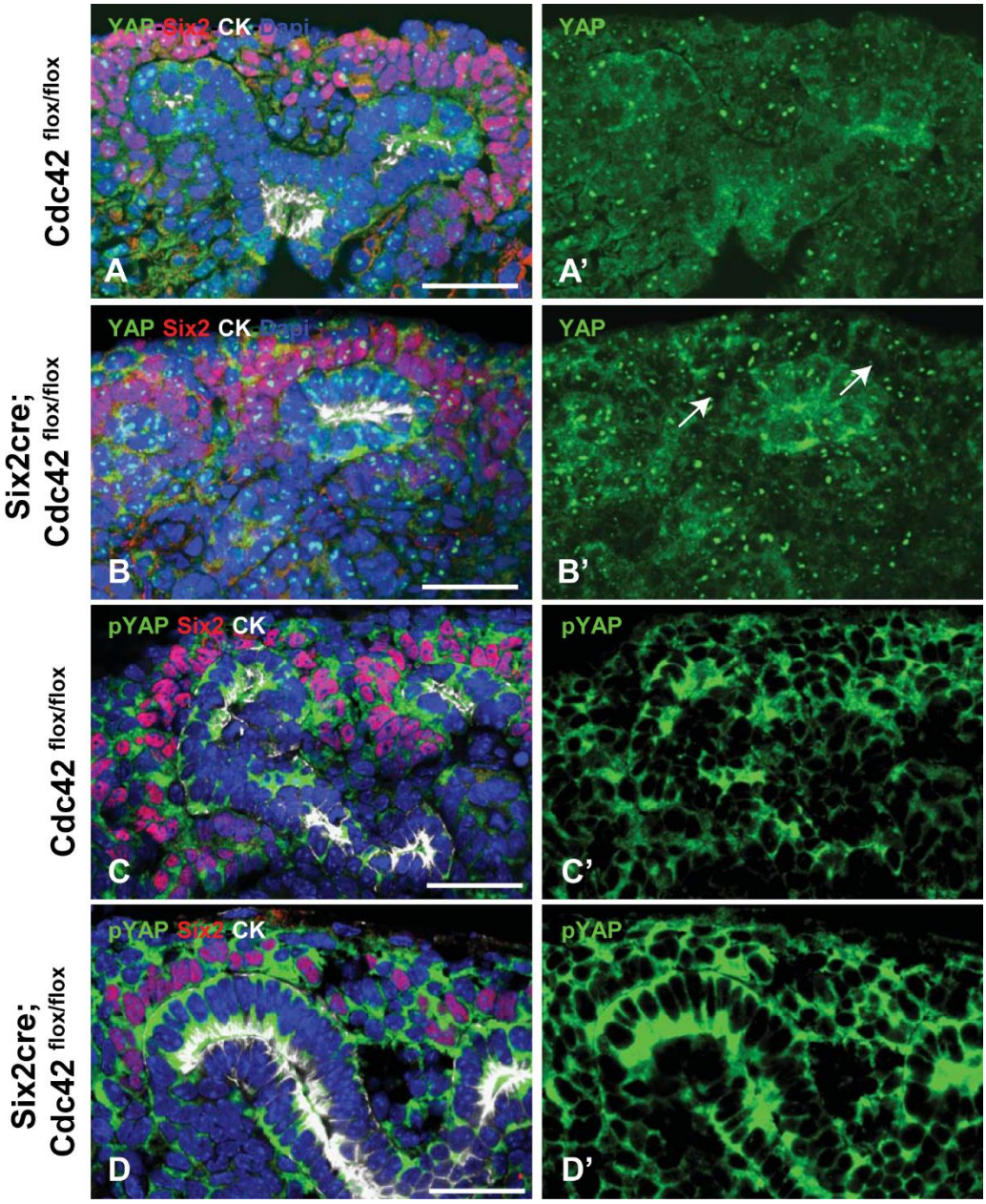

Supplemental Figure 4. E 15.5 Cdc42$^{flox/flox}$ (A, C) and Six2-cre;Cdc42$^{flox/flox}$ kidneys are analyzed for the expression of YAP (green in A, A', B, B') and the phosphomimetic form of YAP, pYAP (green in C, C', D, D'). The nephron progenitor cells are shown with Six2 in red and the collecting duct structures with CK in white A, B, C, D. Arrows in B show decreased YAP expression in the MM of Six2-cre;Cdc42$^{flox/flox}$ kidneys. Scale bars: 50 μm.